Synthesis of PAM and Na-Ac/AM Hydrogel-Coated Mesh for Separation of Oil/Water Mixtures

by

Amal Alsubaei

A thesis
presented to the University of Waterloo
in fulfillment of the
thesis requirement for the degree of
Master of Applied Science
in
Chemical Engineering (Nanotechnology)

Waterloo, Ontario, Canada, 2016
© Amal Alsubaei 2016

AUTHOR'S DECLARATION

I hereby declare that I am the sole author of this thesis. This is a true copy of the thesis, including any required final revisions, as accepted by my examiners. I understand that my thesis may be made electronically available to the public.

Abstract

Hydrogels are used in many applications and have gained popularity due to their high water content, good biocompatibility and similarity to soft tissue. The research objective is to design and synthesize self-healing hydrogels in water/oil/gas system targeted for the separation of water from oil-water mixtures. This will be achieved by graft polymerization of water-soluble polymer such as polyacrylamide (PAM) homo-polymer and poly (Na-Ac/AM) copolymer reinforcing on a thin-fine metallic mesh. This work also involves the study of the effect of mesh size on the amount of water recovered from the oil-water mixture. Further, the factors affecting the micro porosity of synthesized hydrogels such as swelling index are investigated. The hydrogel coated percentage and swelling index (a characteristic property of hydrogels that indicates how much water is absorbed by the gel) are investigated. Different experiments are performed using several mesh sizes and various industrial oils. The hydrogel morphology was analysed by using scanning electron microscopy. Experiments conducted provide quantitative data regarding the degree of the separation of oil from water by using hydrogels. PAM Hydrogel- Coated Mesh was fabricated using a photo-initiated polymerization process with acrylamide (AM), N, N'-methylene bisacrylamide (BIS), 2,2'-diethoxyacetophenone (DEOP), and polyacrylamide (PAM) (number average molecular weight is M_n = 5,000,000-6,000,000) as the precursor, cross-linker, initiator and adhesive agent, respectively. Distilled water was used to dissolve the AM, BIS, DEOP and PAM (50,55,60:1.5:1:0.5 by weight) respectively. Furthermore, Poly (Na-Ac/AM) Hydrogel-Coated Mesh was fabricated also by a photo-initiated polymerization process with sodium acrylate (Na-Ac), acrylamide (AM), N, N'-methylene

bisacrylamide (BIS), 2,2'-diethoxyacetophenone (DEOP), and polyacrylamide (PAM), as co-monomer, precursor, cross-linker, initiator and adhesive agent, respectively. In these copolymer hydrogels, distilled water was used to dissolve the Na-Ac, AM, BIS, DEOP and PAM (10,55,50,5:1.5:1:0.5 by weight) respectively. The effect of the copolymer concentration on the separation time was studied through changing the monomers and the water concentrations. Oil-water mixtures of 5/95, 10/90 and 30/70 Oil/Water % were chosen based on industrial practices as it is not typical to find a wastewater stream with more than 30% oil composition. In all cases, water passes through the mesh, whereas the oil remained in the upper glass tube. Any remnant oil that existed in the permeated water inside the beaker was analysed with an oil analyser. The wettability of water and oil on the PAM- hydrogel coated mesh was evaluated using the contact angle measurements obtained at ambient temperature. It was found that PAM polymer and Na-Ac/AM copolymer hydrogel coated meshes is a super-hydrophilic in an air-solid-liquid three phases with both the contact angle of oil and water lower than 15 degree and in under-water membrane become highly repulsive for oil, where all underwater OCAs of the four different size of meshes based on PAM coated mesh are greater than 90 degree. This indicates the hydrophobic properties of the coated mesh under the water and oil cannot penetrate through the coated mesh while the water absorbed through it. The difference in the water flow or separation time becomes smaller with increasing the mesh's pore size up to 80 micron, while separation time was higher for 200 micron mesh as more hydrogel was as hydrogel was blocking the pores. In contrast, the separation time is faster with the copolymer due to the higher swelling capacity of the copolymer. Therefore, under-water oleo-phobic properties of the PAM coated mesh make it a promising candidate for many applications, such as for wastewater treatment

produced in industry and daily life with more than 95% separation efficiency. However, Na-Ac/AM copolymers coated meshes have lower separation efficiency than PAM homo-polymer due the highest swelling capacity of copolymers hydrogels, which end up with taking off from the mesh.

ACKNOWLEDGEMENTS

I am grateful to reach my milestone in my life. First and foremost, I would like to take this opportunity to thank and express my sincere gratitude to my supervisors, Professor Chandra Madhuranthakam and Professor Ali Elkamel, for their encouragement, invaluable guidance and advice, constructive criticism and support in the difficult period of the study and preparation of the thesis.

Secondly, I would like to thank Prof. Aiping Yu and Prof. Ting Tsui, and it is a great opportunity to have them as thesis committee members. Moreover, I would like to thank Prof. William Anderson for his support with UV light and Prof. Pu Chen for his support with contact angle measurements.

I would like to thank the watlab members Dr. Shantinarayan Rout and Dr. Anisur Rahman for the guidance, availability and help to do the UV-VIS part of work, Dr. Kaveh Sarikhani for his help with measuring contact angles and Dr. Saurabh Srivastava for help with SEM images. Moreover, I would like to acknowledge Dizhu Tong for his help, advice and support.

I would like to deeply acknowledge my husband Bandar Alsahli, my kids Juwana and Saif, and my parents for their endless support throughout my studies. Without their support, I could not be able to complete my studying. Most of all, I am deeply grateful to my sister and brother for their support with taking care of my kids through my studying. Last but not least, I am grateful to my friend Khalsa Alhusaini for the consistent encouragement and help all the way long.

Dedication

To my dear parents and my husband, for their never-ending love and support

Table of Contents

List of Figures

List of Tables

List of Abbreviations

Acronym	Full name
ASTM	American society for testing and materials
°C	Degrees Celsius
cm	Centimeter
cm3	Cubic centimeter
g	Gram
hr	Hour
Kg	Kilogram
m	Meter
MPa	Megapascal
rpm	Rounds per minute
T	Temperature
Wt.%	Weight percent
SWCNTs	Single Wall Carbon Nano Tubes
API	American Petroleum Institute
PPY	Poly Propylene
AM	Acrylamide
PAM	Polyacrylamide
BIS	N, N'-methylene bisacrylamide
DEOP	2,2'-diethoxyacetophenone
DI	Distilled
Na-AC	Sodium Acrylate
SSM	Stainless steel Mesh
SEM	Scanning Electron Microscopy

HCP	Hydrogel Coated Percentage
PPY	Polypyrrole
CA	Water Contact Angle
OCA	Oil Contact Angle
$(\boldsymbol{V_{water}})_{\boldsymbol{filtrate}}$	Volume of water present in the filtrate
$(\boldsymbol{V_{water}})_{\mathbf{0}}$	Volume of water in initial feed mixture
$(\boldsymbol{V_{oil}})_{\boldsymbol{filtrate}}$	Volume of oil present in the filtrate
$(\boldsymbol{V_{oil}})_{\mathbf{0}}$	Volume of oil in initial feed mixture

Chapter 1: Introduction and Objectives

1.1 Motivation

It is estimated that 20 billion barrels of wastewater per year are produced by the oil and gas industry in the US alone.[1,2] Therefore it can be seen that oil/water separation is an important issue that many industries have to address. With the growing need to process oil and water mixtures, new innovative techniques to separate oil from water are desired. Moreover, one of the worldwide challenges is oil/water separation because of increase in the oil spill and industrial wastewater. Therefore, the objective of this research project is to design and synthesis of self-healing hydrogels targeted for separation of oil from water. The first goal was to determine if hydrogels could be applied in these processes, and this was done based on three different monomer concentrations.

Hydrogel describes three-dimensional network structures which are obtained from synthetic or natural polymers and are defined as cross-linked polymeric materials that can adsorb significant amounts of water and swell within its structure, however, it is not soluble in water.[3–5] Over the last few decades, synthetic hydrogels attracted more industrial and research attention than natural hydrogel, due to their high water absorbance capacity and content, higher mechanical strength, and longer life-time. Furthermore, it is possible to change the chemistry of the hydrogel by controlling its surface properties, polarities, mechanical properties and swelling behaviour.[3–5] Hydrogel can also be stimuli to surrounding environment such as temperature, pH and light. Materials, methods and process that are used to produce hydrogel and its classifications are extensively reviewed by H. Gulrez and M. Ahmed.[3,4] Since

hydrogels have excellent hydrophilic surface, they are used in many applications and have gained popularity due to their high water content, good biocompatibility and similarity to soft tissue.[6] Polyacrylamide hydrogel has been used in many fields such as agriculture, tissue engineering,[4,7] pharmaceutical,[4,5,7] biomedical fields,[3,7] water treatment for heavy metal removal,[8,9] and plugging agent for enhanced oil recovery[10,11]. Crosslinking is the most important influence of the polymer and has a large number of applications because it can improve the thermal and the mechanical prosperities of both preformed and bulk materials, where linking process results in increasing the size of the branched polymer with decreasing solubility.[4] Water-soluble hydro-phobically polymers such as polyacrylamide polymer are an area of interest in many industrial applications such as paints, cosmetics, oil recovery and drilling fluids due to hydrophobic co-monomer containing alkyl and aryl distributed acrylamide which enhances the thickening properties and air-liquid surface activities. While there are currently membrane-based technologies that can be used to separate these oil/water mixtures they often have drawbacks, such as requiring high-energy inputs or expensive equipment.[12] An appealing technology that could be used to meet this demand is hydrogels. For the application of treating oil wastewater, hydrogels can be engineered to be oleo-phobic and hydrophilic. The hydrophilicity allows water to easily pass through the hydrogel, while the oleophilicity prevents oil from entering or passing through the hydrogel.

1.2 Objective

The objective of the research is to design and synthesize self-healing hydrogels targeted for separation of oil from oil-water mixtures and will focus on the properties of hydrogel. This will be achieved by graft polymerization of water-soluble polymer such as PAM polymer and (Na-Ac/AM) copolymer and reinforcing on to a stainless

steel mesh (SSM). Experiments are conducted to provide quantitative data regarding the degree of the separation of oil from water by using hydrogels. This work also involves the effect of the mesh size on the amount of water recovered from the oil-water mixture. Further, the factors affecting the micro porosity of the synthesized hydrogels such as the monomer amount in the hydrogel are investigated. The effects of the monomer amount in hydrogel on swelling ratio are studied. The hydrogel morphology was analysed by using scanning electron microscopy SEM.

1.3 Outline of thesis

This thesis consists of six chapters. The scope of each chapter is listed as follows:

Chapter 1 gives an introduction to polymer hydrogels and their behavior with respect to oil/water separation. The objective of the research and the outline of the thesis are presented in this chapter.

Chapter 2 provides a review of the literature on the preparation of polymeric hydrogels, separation mechanism, various membranes and hydrogels that were used for oil/water separation and oil/water determination.

Chapter 3 describes the experimental work related to the synthesis of reinforced PAM hydrogel and (Na-Ac/AM) copolymer hydrogel.

Chapter 4 presents results and discussions of this study including, (1) water recovery, (2) separation efficiency (3) separation time, (4) wettability, (5) swelling ratio, (6) hydrogel coated percentage, (6) and morphological characterizations.

Chapter 5 states general conclusions, which are drawn from this study and recommendations for further studies.

Chapter 2: Literature Review

2.1 General Introduction of Polyacrylamide

Polyacrylamide (PAM) is a white, brittle odourless polymer that can be synthesized by free radical polymerization of acrylamide monomer with the molecular formula C_3H_5NO. Its chemical formula is illustrated in Figure 2.1. PAM is synthetic polymer; therefore, it is used widely to improve commercial products and processes. It is a water-soluble polymer at all concentrations, pH values and temperatures.[3,4]

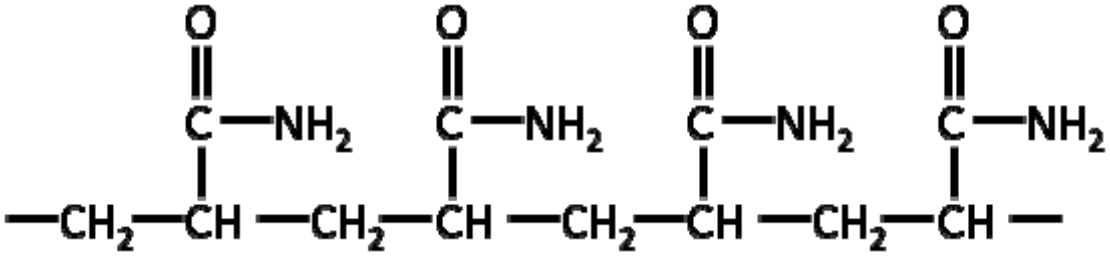

Figure 2.1. Chemical formula for poly(acrylamide) polymer.

One of the most important material properties of liquid is viscosity. PAM viscosity in water increases dramatically with molecular weight, while it decreases with increasing temperature.[13] PAM is one of the most widely used polymers in the world. One of the most important applications of PAM is in enhanced oil recovery.[14]

2.2 Free Radical Polymerization

Polyacrylamide hydrogel is usually synthesized by free radical polymerization, which involves four steps: initiation, propagation, chain transfer and termination. The mechanism of free radical polymerization has already been studied in literature, which is shown in Table 2.1.[15]

Table 2.1. Free Radical Polymerization Mechanisms

Steps	Mechanism
Initiation	$I \xrightarrow{\text{kd}} 2R^*$ $R^* + M \xrightarrow{K_i} M_1^*$
Propagation	$M + M_1^* \xrightarrow{K_p} M_2^*$ $M + M_i^* \rightarrow M_{i+1}^*$
Chain transfer to monomer	$M_i^* + M_1 \xrightarrow{K_m} M_1^* + P_r$
Chain transfer to solvent (S)	$M_i^* + S \xrightarrow{K_S} S^* + P_r$
Chain transfer to chain transfer agent (CTA)	$M_i^* + CTA \xrightarrow{K_{CTA}} CTA^* + P_r$
Chain transfer to impurity or inhibitor (I)	$M_i^* + I \xrightarrow{K_I} I^* + P_r$
Termination by combination	$M_n + M_m \xrightarrow{K_{tc}} M_{n+m}$
Termination by disproportionation	$M_n + M_m \xrightarrow{K_{td}} M_n + M_m$

As shown in Table 2.1, polymerization starts with initiation step that involves the decomposition of an initiator and the initiation of a monomer forming a monomer free radical. The rate of free radical production, R_i, can be shown in equation (2.1)[15] as following.

$$R_i = 2fK_d[I] \tag{2.1}$$

Here, f is the initiation efficiency, which ranging from 0 to 1, while K_d is the initiator decomposition rate constant and [I] is the initiator concentration. According to equation (2.1), the initiation rate is proportional to the initiator efficiency and initiator concentration at a fixed temperature. The next step is propagation that usually leads to

increase in the polymer chain length. The radicals react with monomer electron pair that are held between two carbons with a sigma bond and propagate one with others.[15] Assuming that the rate of propagation does not depend on the chain length, it can be shown as follows.

$$R_p = K_p[M^*][M] \tag{2.2}$$

Third step is termination where free radicals are terminated by a combination or disproportionation. The rate of termination is given by the following.

$$R_t = 2\ K_t[M^*]^2 \tag{2.3}$$

Here, K_t is the termination rate constant and $K_t = K_{tc} + K_{td}$, where K_{tc} and K_{td} are the termination rate constants for combination and disproportionation respectively. With steady state assumption the concentration of free radical remains constant, i.e., $\frac{\mathrm{d}\,[M^*]}{d_t} = 0$, and $R_t = R_i$. Therefore, free radical concentration can be obtained from the following equation.

$$[M^*] = \left[\frac{fK_d[\mathrm{I}]}{K_t}\right]^{1/2} \tag{2.4}$$

Combining equations (2.4) and (2.2) leads to equation (2.5).

$$R_P = K_p\left[\frac{fK_d[I]}{k_t}\right]^{1/2}[M] = \frac{k_p}{K_t{}^{1/2}}\,[\,fKd\,[I]]^{1/2}[M] \tag{2.5}$$

Based on this mechanism, the overall rate of propagation depends on k_p, k_t, k_i monomer and initiator concentrations and initiation efficiency. Moreover, the majority of monomer free radicals are consumed in the propagation step. However, small molecules consume few of them such as impurity, chain transfer agent and solvent that can affect the molecular weight of the final polymer. The corresponding

rates of chain transfer to solvent, chain transfer agent and impurity are given by equations (2.6) to (2.8).

$$R_s = K_s[M^*][S] \tag{2.6}$$

$$R_{CTA} = K_{CTA}[M^*][CTA] \tag{2.7}$$

$$R_I = K_I[M^*][I] \tag{2.8}$$

Here, R_s, R_{CTA} and R_I are the rate of chain transfer to solution, chain transfer agent and impurity, respectively. K_s, K_{CTA} and K_I are the rate constants of chain transfer to solution, chain transfer agent and impurity, respectively. The radicals are transferred to another molecule. Hence, the activity changes.[15] As a result, the molecular weight is decreased.

The mechanism in a copolymer system is simple, which is formed by introducing a second monomer species in the polymerization. The mechanism is shown in equations (2.9) through (2.12).

$$M_1^* + M_1 \xrightarrow{K_{P11}} M_1^* \tag{2.9}$$

$$M_1^* + M_2 \xrightarrow{K_{P12}} M_2^* \tag{2.10}$$

$$M_2^* + M_2 \xrightarrow{K_{P22}} M_2^* \tag{2.11}$$

$$M_2^* + M_1 \xrightarrow{K_{P21}} M_1^* \tag{2.12}$$

In the equations above, M_1^* is the live chain terminated in monomer 1 and M_2^* indicates the live chain terminated in monomer 2. K_{pij} is the rate constant of propagation of adding monomer j to monomer free radical ending with monomer i.

The Mayo-Lewis model is commonly used for copolymerization system, which describes the distribution of monomer in the copolymer. According to the

above-mentioned mechanisms outlined in equations (2.9) through (2.12), the reaction rates of the two monomers can be written as follows.

$$R_{M1} = \frac{d[M_1]}{dt} = K_{p11}\,[M_1^*]\,[M_1] + K_{P21}\,[M_2^*]\,[M_1] \tag{2.13}$$

$$R_{M2} = \frac{d[M_1]}{dt} = K_{p12}\,[M_1^*]\,[M_2] + K_{P22}\,[M_2^*]\,[M_2] \tag{2.14}$$

By dividing these two equations under a quasi-steady state assumption, it yields the Mayo-Lewis equation, which is shown in equation (2.15).

$$\frac{d\,[M_1]}{d[M_2]} = \frac{[M_1]\,(r_1[M_1] + [M_2])}{[M_2]\,([M_1] + r_2[M_2]\,)} \tag{2.15}$$

Here, r_1 and r_2 are the reactivity ratios of the two monomers and defined as in equations (2.16) and (2.17).

$$r_1 = \frac{K_{p11}}{K_{p12}} \tag{2.16}$$

$$r_2 = \frac{K_{p22}}{K_{p21}} \tag{2.17}$$

Generally, the reactivity ratio specifically depends on the reaction conditions such as pH, solvent, monomer species and reaction temperature. These parameters for most of the common monomer combinations can be found in published literature and polymer data/property handbook. For the monomer feed composition in a copolymer can be shown as follows.

$$f_1 = \frac{[M_1]}{[M_1]+[M_2]} \tag{2.18}$$

$$f_2 = 1 - f_1 = \frac{[M_2]}{[M_1]+[M_2]} \tag{2.19}$$

Here, f_1 is the feed composition of monomer 1 and f_2 is the feed composition of monomer 2. Combining equations (2.18) with equation (2.19) yields equation (2.20), which can be used to estimate copolymer composition by using monomer feed composition and reactivity ratio.

$$F_1 = \frac{r_1 f_1^2 + f_1 f_2}{r_1 f_1^2 + 2 f_1 f_2 + r_2 f_2^2} \tag{2.20}$$

Here, F_1 is the monomer instantaneous composition in the polymer mixture.

2.3 Existing Method of Oil/Water Separation

Hydrogel are compared to common existing products and methods to consider its feasibility for this purpose. Table 2.2, summarizes some common technologies used in industries based on the minimum oil particle size to be removed.[16] It can be seen that the methods that use water and oil density differences include API gravity settlers, which use gravity for separation, as well as centrifuges and hydro-cyclones, which both use centrifugal force for separation. Lastly, induced gas floatation with and without flocculants, works by bubbling gas through the solution, causing the oil particles to adhere to the gas and thus, rising to the surface of the solution. Some of the problems that arise using these methods include fouling, the high cost of equipment, low separation efficiency and retention time when the oil droplets are smaller and energy requirenment.[17] For example, a common removal process is the plate separator in the API gravity separator, which helps coagulate the oil droplets for easier removal of oil. However, with the presence and accumulation of solids these parallel plates often require frequent cleaning.

Table 2.2 Common Existing Oil Separation Technologies.[16]

Common Oil Separation Technologies
▪ API gravity separator ▪ Corrugated plate separator ▪ Induced gas floatation (no flocculants) ▪ Induced gas floatation (with flocculants) ▪ Hydro-cyclone ▪ Mesh coalesce ▪ Media filter ▪ Centrifuge ▪ Membrane filter

2.4 Membrane for Oil/Water Separation

2.4.1 Superoleophobic Polymers Surface

Polymers play an important role in synthesized superoleophobic surfaces that can be used to repel oil from water, and they also have unique combination of properties, good biocompatibility and low cost. There are various methods to fabricate polymer with superoleophobic surface that could repel oil. Chiba et al. (2010),[18] and Yan et al. (2007),[19] synthesized new monomers of fluorinated alkylpyrroles, where they achieved a highly oil-repellent film by using electrochemical polymerization. Wang et al. (2011) fabricated pattern-able electrically conductive coatings that have a superhyrophobic and superoleophobic surface, which have been prepared by one-step vapour-phase polymerization of polypyrrole (PPY) in the presence of a fluorinated

alkyl silane directly on fibrous substrates.[20] These treated fabrics can easily repel both oil and water fluids, which can be used in the potential applications of development of intelligent clothing and electronics textiles.[20]

2.4.2 Under-water Superoleophobicity

A superoleophobic surface, explained in the previous section exists only in the absorbance solvent like water. When it is immersed in water, superoleophobicity is lost and their surfaces show superpleophilic nature.[21,22] Under-water superoleophobicity has wide potential applications, like oil-repellent coatings on ships, other marine equipment and in oil spill clean up applications.[3,23] Under-water superoleophobicity in oil/water solid three phase system is challenge and is very important to understand is oil/water separation methods.[10,17,24–26] Oil-repellent coatings for metal[27–29] and textiles, [20,27] are widely used for separation of oil from water, as it can keep the substrate from fouling or corrosion by oils or other liquids, which are commonly used to achieve superoleophobic surface like dip-coating,[10,11,30,31] spin-coating and spray-coating.[23] Fluoropolymers are the most widely used materials because of their good process-ability, flexibility and low cost.[23]

Based on the literature review on hydrophobicity and under-water superoleophobicity, it can be concluded that under-water superoleophobicity can be examined by oil contact angle under-water on the coated surface. Surfaces with hydrophilic and under-water superoleophobic can achieve high oil contact angle under water (greater than 150°). Therefore, due to hydrophilic properties, water is usually trapped in the rough surface of the coated surface. Trapped water repels oil from penetrating and passing through the coated surface, yielding superoleophobic and low adhesive surfaces in water.[23,31]

2.5 Benefits of PAM- Membrane Filter for Oil/Water Separation

The most notable benefit with PAM-membrane filter is that the chances of the hydrogel being fouled by the oil is minimum and there is no oil absorption is observed unlike media filter, and is evident from the hydro-philicity and underwater hydrophobicity of the hydrogel. Moreover, water treatment with conventional filters has the chance of foul over time and eventually need to be replaced and re-cleaned to remain effective for the separation. Therefore, the reduced chance of the hydrogel fouling advocates that the hydrogel could have a longer effective lifetime than other membrane type technologies, which can also be recycled for at least three times with almost the same results.

Another benefit of hydrogels is that the formulation is relatively simple. Hydrogel formulation for the purposes of this project required only four chemical ingredients as well as deionized water and a stainless steel mesh. The procedure for synthesizing the hydrogel is also a relatively simple process, as will be discussed later in chapter three. The operational costs of using hydrogels would be very low compared to many of the other methods. Also, unlike centrifuge, using hydrogels only energy required is for pumping the fluid. These are environmentally friendly with less toxicity of the final hydrogel product. Moreover, it is very effective for small oil particles, small emulsifications and small mesh sizes.

In the wastewater treatment the hydrogel is grafted onto a stainless steel mesh for structural integrity and the mesh size can be varied according to the type of application.

Hydrogels are an ideal alternative to the conventional technology of treating oil water waste streams due to their resistance to fouling, low production and operational costs and easy customizability.

2.6 Sodium Acrylate/Acrylamide Copolymer

Mohana et al. (2001) had investigated superabsorbent polymer (SAP), where the preparation is based on using acrylamide, acrylic acid, and its salts by inverse-suspension polymerization and diluted solution polymerization.[32] The superabsorbent polymer that has the ability to absorb water or aqueous solutions up to hundreds of times of their original weight, are water-insoluble three-dimensional cross-linked network structures of hydrophilic monomers and has been used in personal hygiene products such as diapers, sanitary napkins, and adult incontinence products.[33,34] There are some of the applications for SAPs such as contact lenses in the biomedical field, food packaging, water purification,[29,32,34] and improvement of water retention of soil.[32] The polymerization was carried out for 2 h under N_2 bubbling at 80 ℃. Swelling of SAPs varied with the relative content of AM and Na-Ac.[34–36] The swelling capacity of the SAPs increases with increasing crosslink density, which reaches a maximum at an optimum crosslink density, and then decreases as the network becomes denser.[36,37] Kalaleh et al. (2015), investigated the influence of the environmental parameters on water absorbency of the Na-Ac/AM copolymer such as the pH and the ionic force, they found that the water absorption decreased with increasing the ionic strength of the saline solution even with increasing the concentration of the ionic strength, as when NaCl concentration increases the absorbency decreases; the reason for this is that ions in the solution decrease the osmotic pressure difference or the driving force for the swelling between the hydrogel

and the solution.[36] Moreover, it was stated that with at low pH, the swelling ratio of Na-Ac/AM copolymer decrease as the sodium carboxylate group on the polymer are protonated and hydrogel shrink and become more hydrophobic. On the other hand, at high pH, the swelling index decreases due to the effect of excess sodium ion in the swelling media, which blocks the carboxylate anion and prevents the effective of anion-anion repulsion. Therefore, for pH from 4 to 8, some of the carboxylic acid groups are ionized and the electrostatic repulsion between them produce improvement of the swelling ratio.[34,36,38]

Therefore, the most widely used method for the synthesis of water-soluble polymer and hydrophilic gels is acrylamide with N-substituted derivations, which has a lot of applications in many fields. For removal of heavy metal ions from natural water and wastewater in industrial and ecological treatment process, sodium acrylate co-monomer is widely used.

Hydrogels containing amide, amine, carboxylic acid, hydroxyl, and ammonium groups can be used for separation of heavy metals such as Cu, Cd and Fe ions from their aqueous solutions, where these groups can bind metal ions and is good for water purification applications.[35] For example, anionic Acrylamide-based hydrogels such as cross-linked acrylamide (AM) and 2-acrylamido-2 methylpropanesulfonic acid (AMPS) homo-polymers and copolymers are prepared by free radical solution polymerization by using N, N-methylene bisacrylamide (BIS) as the cross linker.[9] Therefore, hydrogels which have one or more electron donor atoms such as N, S, O and P can form coordinate bonds with most toxic heavy metals.[9,35,39] Krušić et al. (2012) investigated hydrogels based on acrylamide and sodium methacrylate regarding their swelling behavior for removal of ph^{2+} from wastewater. [40] It was found that the swelling behavior and the removal capacity, both increase by

increasing the amount of sodium acrylate.[40]

Many industries including electroplating, lead batteries, paint and dyes, and glass operation are sources of heavy metal waste.[9,41] The excessive amount of heavy metals including lead, arsenic, chromium, mercury, copper and zinc contribute to the hazardousness of wastewater.[41] It is important to reduce the amount of heavy metals in the wastewater as they lead to toxicological effects to the environment and to human health. Therefore, they must be removed from wastewater and drinking water. High concentration of copper ions found in many wastewater sources creates a kind of disease with similar effect as the flu; [41] the high toxicity of lead can lead to damage of many tissues in living organism; copper can also cause damages to the health of many living organisms.[41] Thus, various methods of removing or reducing heavy metals from solutions have been developed like ion exchange[42], chemical precipitation[43], adsorption[8] and membrane separation[9]. Karadag et al. (2002) prepared super-water-absorbent acrylamide-sodium acrylate hydrogels by free radical polymerization in aqueous solutions of acrylamide with sodium acrylate as co-monomer that can be used for heavy metal removal.[34] In this research project, the acrylamide and sodium acrylate copolymer hydrogel targeted for separation of oil/water system will be investigated in this study.

Zhou et al. (1990) obtained acrylamide-sodium acrylate copolymer hydrogel gel through radiation techniques by using two different methods to introduce –COONa groups into polymer chains of the gels, where these two methods were obtained from partial hydrolysis of acrylamide homo-polymer gel and direct copolymerization and crosslinking of acrylamide and sodium acrylate in aqueous solutons.[33,44] The first method entailed making the AM hydrogel, then hydrolyzing it by a basic solution (0.5 M Na_2CO_3), where the $-CONH_2$ group in AM polymer

converts to a -COONa group. The water retention volumes (WRVs) of AM polymer was quite small, but once hydrolyzes it increased a hundred times due to the formation of the –COONa group, which is much more hydrophilic than –CONH2 group.[33] A similar effect was reported previously that Na-Ac is superabsorbent.[33,34,44,45] Zhou et al. (1990) studied the affect of pH on the WRVs. Whereas AM hydrogels were almost independent of pH before hydrolysis, WRVs of acrylamide-sodium acrylate copolymer were dependent on pH.[33] When PH was below 2, WRVs were very small and increased slightly with increasing pH.[33] Moreover, when a swollen gel is added to an acid solution, the gel began to shrink and released the absorbed water due to a decrease in the pH level. However, when basic solution is added to the shrunken gel, it would swell up again by absorbing water.[33] These can be explained by the electrostatic interaction of $-COO^-$ group in the polymer chain resulting from the ionization of –COONa groups, as shown in equation (2.21).[33]

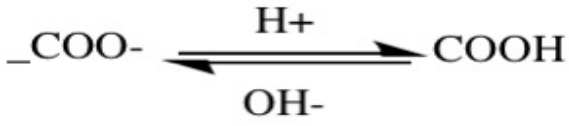

(2.21)

Magalhães et al. (2012) observed that more acrylamide was found in the hydrogel than sodium acrylate (50 %v/v for each). This was because sodium acrylate polymerizes less readily, as ionized monomers react more slowly in the propagation step of polymerization.[44] The results found for poly (sodium acrylate-co-acrylamide) hydrogels indicate that acrylamide is around 20% more reactive than sodium acrylate, where the reactivity consequence seems to follow the order: acrylamide > sodium acrylate > acrylic acid.[33,44,45] Anionic hydrogels based on sodium acrylate (Na-Ac) and acrylamide (Am) are well known, extensively studied and produced on a large scale.[44]

2.7 Graft Polymerization of Polyacrylamide

Polyacrylamide is synthesized using monomers, cross-linkers and initiators. The proportion of components affects the rate of polymerization and the swelling behaviour of the polymer. The rate of polymerization and the properties of the final hydrogel also depend on the concentration of the initiators.

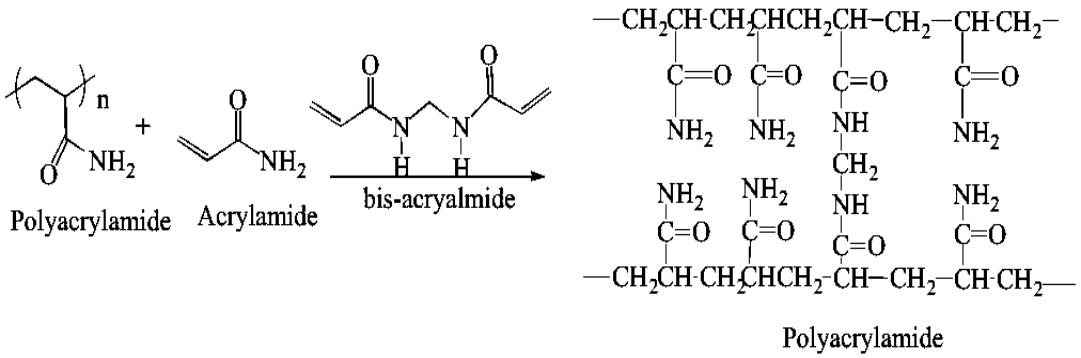

Figure 2.2 Chemical formulas of polymerization of polyacrylamide polymer.

2.8 Oil/Water Determination Methods

Detection of oil is a tedious and a slightly sophisticated analytical technique, where gas chromatography (GC), HPLC and gravimeter were used in general. In contrast, UV-NIR provides fast and non-destructive measurements with no sample preparation.[46] Therefore, the concentration of oil in the wastewater is a method-dependent parameter, which is traditionally evaluated using reference methods based on infrared (IR) absorption or gravimetric analysis, Gas Chromatography and Flame Ionization Detection (GC-FID).

Gravimetric-based methods can be used to measure anything that is extractable by a solvent that is not removed during a solvent evaporation process and

is capable of being weighed. In this method, oil/water is extracted by a solvent such as hexane and then separated by a funnel separator. After separating the solvent containing the oil from the water sample, it is transferred into a flask, which has been weighed beforehand. Then, the solvent needed to be evaporated at a specific temperature by placing the flask into a temperature controlled water bath. After evaporating of the solvent, the flask now just contains the residual oil. The amount of oil can then be calculated by drying and weighing the residual oil.[47] However, one of the drawbacks of this method is that the procedure must be carefully controlled, is time consuming and is not suitable for very small amounts of oil.[48]

In an UV-VIS-NIR based method, the oil/water sample needs to be acidified, and extracted by organic solvents that can be used to extract oil from water such as n-hexane, CCL_4 or dichloromethane.[47] The extraction solvents play an important role in these methods, where they are used to extract oil from a water sample. Various solvents can be used for extraction. A good solvent should possess a number of properties in addition to having good extraction ability. Some of these properties are as follows: sufficient infrared transmission (infrared transparency), environmentally friendly, safe to use, reasonably priced, easily available, and heavier than water, which means that they can be easily separated from the water phase and drained from the extraction funnel.[47] The extracted oil is then removed, dried and purified by the removal of polar compounds using dry agents such as sodium sulphate to absorb any moisture. Furthermore, anything that is not extracted will not be included in the analysis. A portion of the extracted oil is placed into an infrared instrument, where the absorbance is measured.

Vegetable oils structurally are mixtures of natural fatty acid esters.[49] According to the literature,[50,51] soybean oil is composed by about 15.1% of saturated

fatty acids (mainly palmitic and stearic acids) and about 83.5% of unsaturated fatty acids (mainly oleic, linoleic and linolenic acid). Therefore, the main spectroscopic properties of vegetable oil will be related with the C-O, C=O and C=C functionalities. The UV-Vis spectra were performed in *n*-hexane because its expected absorption bands are less than 200 nm, being a saturated hydrocarbon. Absorption bands over 200 nm should exclusively be generated by the samples of oil. Both UV and visible method can be used for measuring oil concentration in water. The UV absorption spectra of oil, often observed to peak at 200-280 nm, which is typical for condensed benzene ring. In addition, another band can be observed in the range of 200-210 nm for ester carbonyl group that present in some oil components. However, for visible wavelength, oil should be coloured enough to absorb visible radiation after the extraction. On the other hand, if oil is colourless, it must contain aromatic hydrocarbon to estimate by UV light.

Chapter 3: Oil/Water Separation by PAM and Na-Ac/AM Hydrogel Coated-Mesh

3.1 Methodology

The methodology of the experiment will be focused on the product design of the reinforced hydrogel. In this chapter the experimental setup, monomer and co-monomer compositions will evaluated. Regarding the hydrogel product, the methodology consisted of several steps in order to synthesize the product and perform testing to determine its viability. Initially, the product (PAM) had to be prepared from four base chemical ingredients and reinforced onto a stainless steel mesh, while (Na-Ac/AM) was prepared from five base chemical ingredients. The product's performance was tested by separation experiments to study the different characteristics of the hydrogel.

3.1.1 Materials

The homo-polymer Polyacrylamide (PAM) (average M.W. 5,000,000-6,000,000) was of laboratory grade in the form of powder. It was purchased from Poly Science, Inc. (Warrington, PA, USA). Acrylamide (AM), which is a white crystalline solid (with M.W. 71.08 g/mol that is suitable for electrophoresis, >99%, A8887-100G), Sodium Acrylate (Na-Ac), N, N' Di-methylene Bisacrylamide (BIS), (for electrophoresis, >99.5%), and 2,2'Diethoxyacetophenone (DEOPS) (>95%) were purchased from Sigma-Aldrich (Oakville, Ontario, Canada). Distilled water was used in all experiments. Stainless steel meshes were purchased from TWP Inc. (Berkeley, CA, USA) in five different sizes—25, 55,65,80 and 200 micron. Glass tubes were ordered from Chemglass Life Sciences (Vineland, NJ, USA), CG 124 with the pinch clamps, (O-Ring Joint, 25mm ID, 30mm Tube OD, O-Ring Size: 217, Clamp Size:

35). Oil was purchased from a local market store. Sodium sulphate and n-hexane were ordered from Sigma-Aldrich for extraction and drying purposes.

3.2 Hydrogel Formulation

3.2.1 PAM Hydrogel Formulation

The PAM hydrogel-coated meshes were prepared using a photo-initiated polymerization process with acrylamide (AM), N, N'-methylene bisacrylamide (BIS), 2,2'-diethoxyacetophenone (DEOP), polyacrylamide (PAM) as the precursor to the final product, a cross-linker to aid in the creation of links between hydrogels, an initiator and adhesive agents to reinforce hydrogels onto the mesh. BIS is an important factor in governing the size of the pores of the hydrogel which inturn affects the swelling index of the hydrogel. Cross linker molecules can be incorporated into polymer chains simultaneously, as they form a permanent link between them. As its name suggests, DEOP is a photo initiator, which forms radicals particularly when subjected to UV light. Inside the fume hood, PAM, AM and BIS (0.5, (50,55,60), 1.5 wt. % respectively) were dissolved in (47, 42 and 37 wt. %) distilled water in that proportion in order in 50 ml glass beaker at room temperature to make three different polymer concentrations based on AM wt. %. The water was first bubbled with nitrogen gas for 15 minutes in order to remove any oxygen from it, which act as an inhibitor and kills the monomer, thus destroying the polymer or potentially initiate the polymerization, which is undesirable at this stage. The proportions of these chemicals are summarized in Table 3.1. Solution was stirred for 1 hour with the mixer turned on to a rotational speed of 600 rpm, and the same mixer speed was used for every experiment for consistency. It was observed that with an increase in the monomer concentration, it takes a longer time to make homogenous solution. Lastly, DEOP

with 1 wt.% was dissolved in the solution and is mixed for 15 more minutes to ensure every composition in the mixer and all the chemicals are dissolved. For each batch, a total solution weight of 40.0g was made, which was used for coating three stainless steel meshes. Since DEOP is photosensitive, it was added in the last to avoid any early onset polymerization. Once the chemicals were added, the solution was covered completely using an Aluminium foil because it is sensitive to light and to protect against polymerization of photo-initiation as shown in Figure 3.1. The same formulation was used throughout all of the experiments to produce three different hydrogel concentrations. The proportion of chemicals used to prepare the hydrogel was consistent each time a solution was made.

Table 3.1 Formulations for Hydrogel Solution.

Ingredient	**% Proportion (by weight)**
Acrylamide	50/55/60
Polyacrylamide	0.5
N, N'-methylene Bis-acrylamide (BIS)	1.5
2,2'-diethoxyacetophenone (DEOP)	1
DI-Water	47/42/37

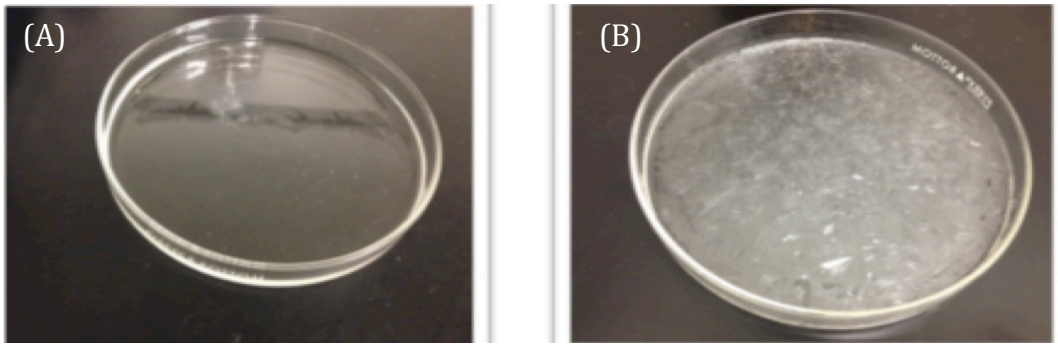

Figure 3.1. Sensitivity of PAM Hydrogel. A) Homogenous solution of the hydrogel. B) Hydrogel exposed to light.

3.2.2. Synthesis of (Na-Ac/AM) Copolymer

Synthesis of poly (Na-Ac/AM) copolymer hydrogel is relatively simple, which consists of five chemicals with the base of the hydrogel being (AM), (Na-Ac/AM), and other chemicals being similar to pam system. Table 3.2 illustrates the chemical formula of Na-Ac, AM and BIS. The Poly (Na-Ac/AM) co-polymer hydrogel was prepared using a photo-initiated polymerization process with AM, Na-Ac, BIS, DEOP, and PAM as the precursor to the final product, a co-monomer, cross-linkers to aid in the creation of links among hydrogels, an initiator and an adhesive agent to reinforce hydrogel onto the mesh once it is polymerised.

PAM, AM, Na-Ac and BIS (0.5, (5/45), (55/10), 1wt. % respectively) were dissolved in (37/42 wt. %) distilled water at room temperature to make two different co-polymer concentrations based on AM and Na-Ac wt. The water was first bubbled with nitrogen gas for 15 minutes to remove any oxygen, as it can cause inhibition during free radical polymerization, which is not desirable at this stage. The proportions of these chemicals are summarized in Table 3.3. The solution was stirred using a magnetic stirrer bar for 1 hour at 600 rpm, and the same mixer speed setting was used for every experiment for consistency.

The copolymer with 10 % Na-Ac dissolved completely in one hour. However, it was observed that increasing the monomer concentration required longer time for mixing to have a homogenous solution. For instance, the copolymer with 55 % Na-Ac took five hours to be dissolved completely. Lastly, DEOP was dissolved in each solution for 15 more minutes to ensure homogenous composition in the mixer. For each batch, a total solution weight of 40.0g was prepared and was used for coating of three stainless steel meshes.

The remaining procedure is the same as that used in the synthesis of PAM hydrogel, where the solution is mixed well using a magnetic stirrer for obtaining a homogenous solution, solution needed to be covered completely by Aluminium foil while mixing in order to prevent UV irradiation from light. Therefore, the same formulation was used throughout all of the experiments in order to produce two different hydrogel concentrations. This ensured that the proportion of chemicals used in preparing the hydrogel was consistent each time a solution was made.

Table 3.2. Monomer, co-monomer and cross-linker used in the preparation of hydrogel system

	Type	**Formula**	**Abbreviations**
Acrylamide	Monomer	H_2C= $CHCONH_2$	AM
Sodium Acrylate	Co-monomer	H_2C= CHCOONa	Na-Ac
N, N-methylene bisacrylamide	Cross-linker	$(H_2C$= $CHCONH)_2CH_2$	BIS

Table 3.3 Formulations for Na-Ac/AM copolymer Solution

Ingredient	**% Proportion (by weight)**
Acrylamide	5/45
Sodium Acrylate	55/10
Polyacrylamide	0.5
N, N'-methylene bis-acrylamide (BIS)	1.5
2,2'-diethoxyacetophenone (DEOP)	1
DI-Water	37/42

3.3 Procedure and Experimental Apparatus

3.3.1 Fabrication of Hydrogel-Coated Mesh

Once the polymer or copolymer solution turned into a homogenous solution, it is then poured into a square dish for easy coating of the mesh pieces. The pre-cleaned mesh was then carefully immersed in the solution for about 5 seconds before it was drawn out slowly and horizontally with the solution adhered to the surface of the mesh, as shown in Figure 3.2. The mesh was removed horizontally and utmost care was taken decreasing the chance of the solution dripping off the mesh.

After dipping, the mesh was irradiated by UV light (360 nm) for 90 min to fully polymerize the solution. This allowed photo-initiation of the coated solution in order to transform it into the polymerized hydrogel. The lamp height (measured from the top of coated mesh surface to lamp surface) was controlled at 5 cm. After polymerization, the coated mesh was washed with distilled water to remove impurities left from the preparation process. These include unreacted monomers, cross-linkers, initiator and other products produced via side reactions. Thus, the final hydrogel-coated mesh was obtained. Fabrication of PAM polymer and Na-Ac/AM copolymer meshes uses the same procedure.

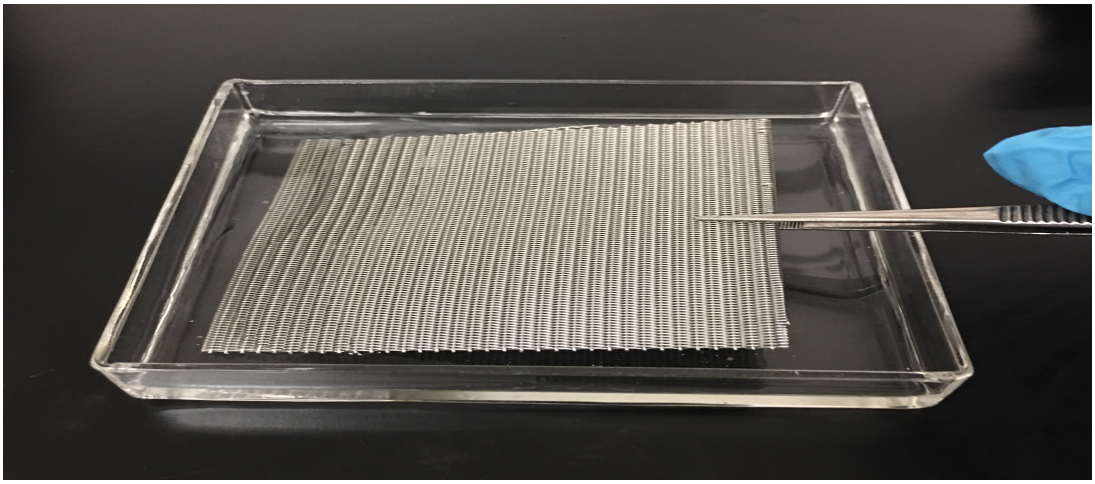

Figure 3.2. Dipping of Clean Mesh Horizontally.

3.3.2 Oil-Water Separation Experiment with Hydrogel-Coated Mesh

The as-prepared coated mesh was fixed between two tube glasses (25 mm in diameter) serving as a separation membrane, and then the oil-water mixture (v/v %) was poured onto the upper glass tube on the hydrogel-coated mesh. 50 ml of Oil/ water mixture, as shown in Figure 3.3 (A), was prepared by mixing desired quantities of the two components and stirring at 600 rpm for 15 minutes in order to form an emulsion in a beaker. It must be noted that no surfactants or emulsion stabilizers were used during the preparation of the oil/water mixtures. Separation of oil and water was carried out as per the setup illustrated in the Figure 3.3 (B). The water passed through the mesh, whereas the oil remained in the upper glass tube.

Separation time was measured. It is important to tighten the clamp well. Otherwise, the mixture will leak as a result of a poor sealing, as shown in Figure 3.4. The separation was measured from the weight of the liquids. The separation of the oil from the water was carried out using the experimental setup shown in Figure 3.3 (B).

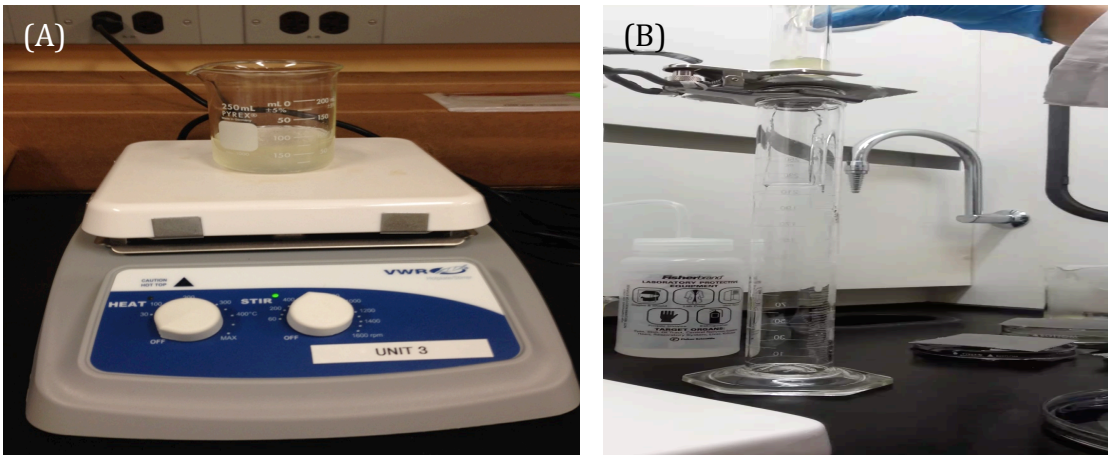

Figure 3.3. (A) Water/oil mixture during mixing and (B) separation process of oil/water mixture

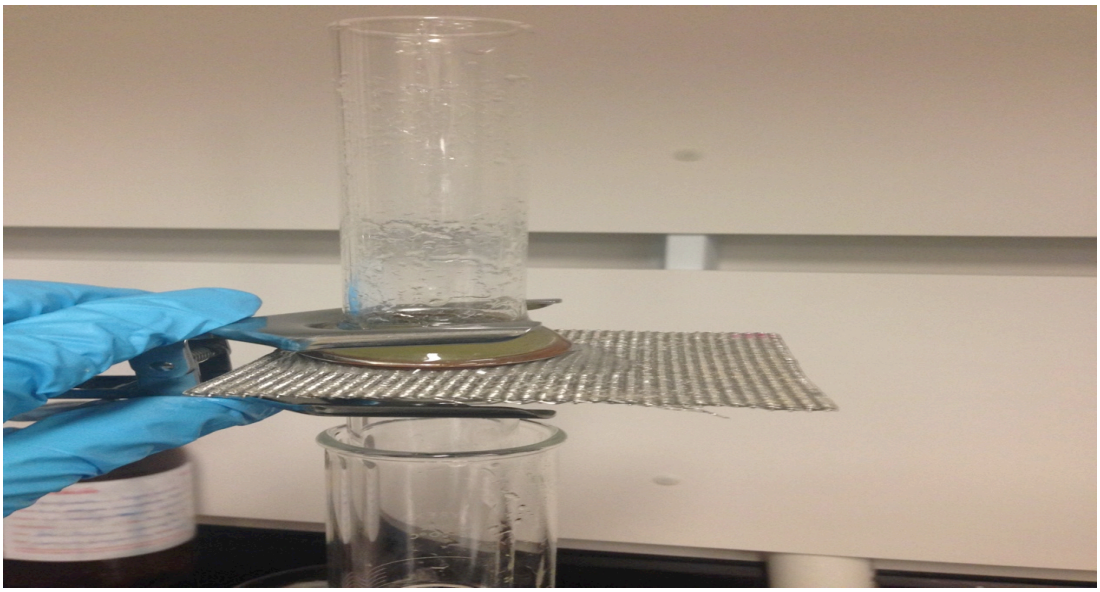

Figure 3.4. Leaking process due to poor sealing. Coated 200-micron mesh with 10% oil was leaking when the sealing was not tight enough

3.3.3 Experimental Parameter

Effect of the polymer and copolymer hydrogel on the separation time is studied by varying the mesh size. Four different pore sizes of the mesh, 55, 65, 80 and 200 micron, are used. As shown in Table 3.4 the oil/water mixture composition was varied at three levels. Oil weight percentages ranging from 5% to 30% are chosen to be tested for PAM and from 5 to 10 % for Na-Ac/A copolymer. Mixtures with higher

oil concentrations can be separated using sedimentors. This range was chosen based on industrial practices, as it is not typical to find a wastewater stream with more than 30% oil composition. Figure 3.5 shows the preliminary experimental design.

Table 3.4 List of Independent and Dependent Variables.

Independent			**Dependent**
	PAM	**Na-Ac/AM**	
• Mesh pore size (micron)	55,65,80 and 200	55, 80 and 200	• Separation Time • Water Recovery • Separation Efficiency
• Oil/Water Mixture Compositions	5/95, 10/90 and 30/70	5/95 and 10/90	
• Monomer %	AM %: 50, 55 and 60	Na-Ac/AM %: 10/45 and 55/5	

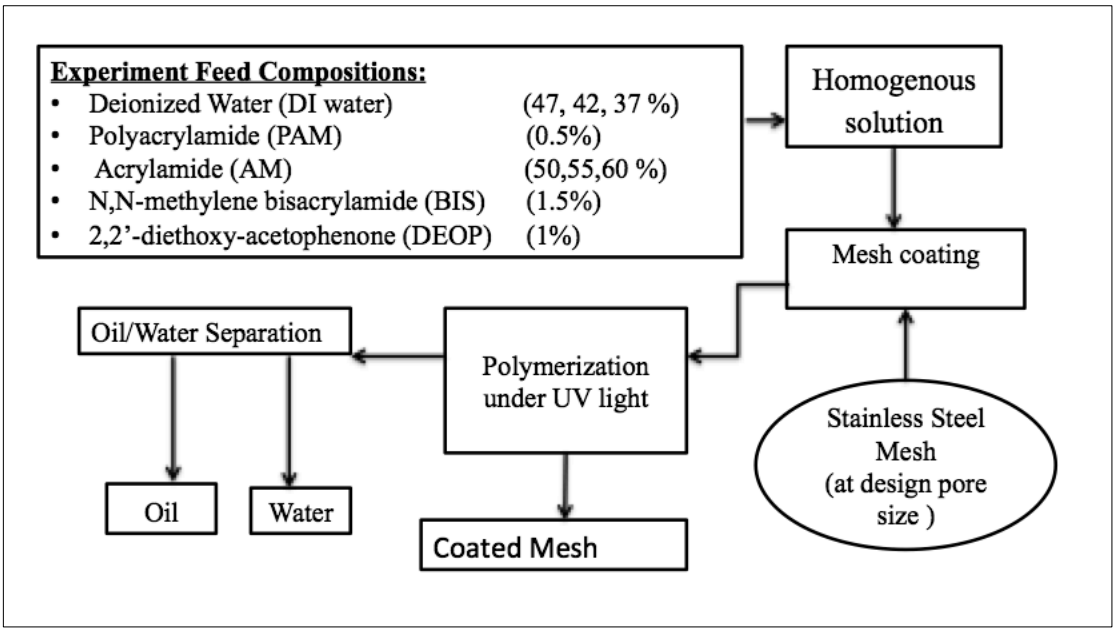

Figure 3.5. Experimental Design Flow Sheet.

3.4 Instrument and Characterization

3.4.1 UV Light

UV light (365 nm) was used to irradiate the sample for approximately 90 to 120 minutes. Aluminium foil was used to cover the UV lamp to create impermeable seal that prevent transmission of UV light outside the unit.

3.4.2 Separation Efficiency

As set of 4X3 factorial experiments with 3 points of repeatability are designed and conducted in which different sizes of mesh, and separation time, reclaimed oil and water recovery are varied.

3.4.2.1 Water Recovery and Reclaimed Oil

After separation, water recovery and reclaimed oil were measured. The water recovery is the percentage of water filtered through the mesh compared to the original water content in the testing mixture by using equation (3.1). In equation 3.1, $(V_{water})_{filtrate}$ is the volume of the water present in the filtrate and $(V_{water})_0$ is the volume of the water present in the initial feed mixture. The reclaimed oil is the percentage of the oil that did not pass through the coated mesh compared to the original oil percentage in the testing sample, which cab calculated equation (3.2), where $(V_{oil})_{filtrate}$ is the volume of the oil present in the filtrate and $(V_{oil})_0$ is the volume of the initial oil in the sample.

$$Water\ Recovery = \left(\frac{(V_{water})_{filtrate}}{(V_{water})_0}\right) * 100\% \quad (3.1)$$

$$Reclaimed\ Oil = \left(1 - \frac{(V_{oil})_{filtrate}}{(V_{oil})_0}\right) * 100\% \quad (3.2)$$

3.4.2.2 Separation Time

Separation time was directly measured during the experiment and required no further calculation. Separation time was recorded from the instant the mixture was poured onto the top glass tube present on the coated mesh until when no fluid droplets were dripping from the bottom of the mesh for at least three seconds.

3.4.3 Contact Angles Measurements

Contact angles of water and oil were measured or characterized using Axisymmetric Drop Shape Analysis-Profile (ADSA-P) with a digital camera at ambient temperature, which is a technique used to determine contact angles, and then transferred to the system.

3.4.3.1 Wettability

To evaluate the performance of the coated mesh in oil/water separation, the under-water oil wettability of the hydrogel is investigated. The wettability of water and oil on the PAM-hydrogel coated mesh was obtained from contact angle (CA) measurements. The oil wettability of the coated mesh was characterized by measuring the CAs of oil underwater with 5 μL droplet of 1,2-dichloroethane (DCE) as the probe liquid that is generated under-water on the coated mesh. The values are reported as the average of at least 4 drops per sample at different random locations. When oil droplets contacted with the PAM coated mesh, the image was captured at room temperature and then the contact angle measured using the ADSA software.

3.4.4 Swelling Index Measurements

To prove and evaluate the utility of the hydrogel's ability as a water holding material, the swelling ratio was investigated as follows (Nagasawa et al., 2004) by using equation (3.3).

$$Swelling\ ratio = \frac{W_s - W_d}{W_d} \quad (3.3)$$

Where, W_s is the weight of the hydrogel in swollen state and W_d is the weight of the hydrogel in dry state. Bulk hydrogel was used to study the swelling ratio, which was synthesised with the same polymer solution. Approximately 1 ml of polymer solution was added to a petri dish and then exposed to UV light for 90 minutes until completely polymerized. The bulk polymer was rinsed with deionized water and then dried using a filter paper. The dried hydrogel is weighed in dry state and again after immersing in known amount of water for 5, 10, 20, 1440 and 2880 minutes. The swelling process was recorded by weighing the hydrogel in dry and swollen state. First, 0.1g of dried bulk polymer was weighed using an analytical scale, and then immersed into deionized water at room temperature within 48 hours to obtain the saturated swollen polymer. The degree of swelling ratio was calculated based on equation (3.3). The swollen hydrogels were removed from water after 5, 10, 20, 1440 and 2880 minutes, wiped with filter paper and then weighed as soon as possible.

3.4.5 Hydrogel Coated Percentage (HCP)

The Hydrogel Coating Percentage was investigated by using equation (3.4)[17].

$$HCP(\%) = \frac{(W_a - W_b)}{W_b} \times 100\ \% \quad (3.4)$$

Where, W_a is the mass of the coated mesh after polymerization and W_b is the original mass of the uncoated mesh before hydrogel immersion. The percentage of the hydrogel-coated mesh was determined based on different mesh pore sizes (55, 65, 80 and 200 micron) for three different monomer concentrations (50, 55 and 60%).

3.4.6 Determination of Oil-in-Water

For controllable separation of oil and water mixtures, the visible oil existed in the permeated water inside the beaker needs to be analysed. To determine oil-in-water

after the separation, a sample had be extracted from the water by solvent extraction, as oil is not soluble in water. For the extraction of oil from the oil/water mixture after the separation, 4.5 mL of the solvent was added to 45 mL of the oil/water samples. These mixtures were stirred and then kept at rest at room temperature as usual in liquid-liquid extraction procedure. Organic solvents such as n-hexane extract oil, which is immiscible in water. Therefore, as n-hexane is less dense than water, the upper phase is the solvent with oil, while the lower phase is the aqueous phase. Separator funnel is used to separate the organic layer from the aqueous layer. After the extraction, it is very important to remove the residual water or moisture from the organic liquid by drying the organic layer containing volatile oil over anhydrous such as sodium sulphate and this can be done by adding the anhydrous to the solvent containing oil. To find how much drying agent to be add, first small amount of the drying agent is added with a spatula because too much of it can absorb the product and the material will be lost. After adding the dry agent, clumping occurs as the anhydrous absorbs water and forms a hydrate. Since majority of the sodium sulphate clumps, it was necessary to add more. If the organic liquid is cloudy, it will turn clear once the organic liquid is totally dried. It was necessary to add more of the drying agent until some of them could be seen not clumped. The sample was left for 5 to 7 minutes to absorb the water from the organic sample.

However, these are only methods to separate the oil from the water, but not to measure the concentration. The oil content was obtained with the help of the calibration curves of the oil in the respective solvent. For the oil measurements, in the separation system, the concentration of the oil after filtration and the separation efficiency were estimated using a UV-VIS spectrophotometer according to a standard procedure. Initially, the absorption spectra of 5 mL of different oil concentrations

(0.0–30.0 mg/L) of oil solutions were recorded after diluting the oil in n-hexane as solvent in the cuvettes. The solvent phase (n-hexane and oil) with unknown oil content was brought to the equipment for UV absorbance reading, which was determined under the same conditions as used to obtain the calibration curves of oil in water. The concentration of oil was calculated by the intensity of the peak and the above-mentioned linear fit. At least two repetitions were made for determining the oil concentration in each sample. Oil concentration in the original sample was calculated by comparing the absorbance that obtained from the extracted sample to those that were prepared with known concentrations. The absorbance value was multiplied by the factor to give a reading in concentration, which is based on the Beer-Lambert law (A=MC), where A is the absorbance, M is the coefficient factor and C is the sample's concentration.

3.4.6 Morphology

3.4.6.1 Scanning Electron Microscopy (SEM)

During the experimental trials on different batches of the hydrogel coated mesh, it was discovered that some meshes would be excellent in passing the water through the mesh, leaving the oil retained at the top. While, some meshes would end up having tiny amounts of oil passing through. Since it was not possible to determine the cause for some mesh that seemed to perform better than others, SEM images of the mesh are investigated. This allowed us to understand possible reasons for varying performance of the mesh and also to see how well the stainless steel meshes were being coated. It is expected that the coating of the mesh would have a strong effect on the result.

SEM was used to provide information about the sample's surface topography. Images were taken with an acceleration voltage from 5 to 10 kV. The test specimens,

which were coated mesh (0.5 cm), were mounted on aluminum stubs with carbon tape. Before starting the measurements, samples were sputter coated with 10 nm of gold using a high-resolution sputter coater.

3.4.6.2 Light Microscopy

The droplet size of oil was obtained by placing 5 ml of the sample under the light microscopy (EVOS fl digital inverted microscope), and 5 images were taken randomly from different areas using a camera microscope. Then, the diameter of the droplets were measured using Image J® software.

Chapter 4: Results and Discussions

4.1 Separation Efficiency

4.1.1 Water Recovery

Water recovery was calculated by using equation (3.1). As we investigated three different amounts of the monomer in the PAM hydrogel and two different concentrations of sodium acrylate in Na-Ac/AM copolymer, we found that water recovery was ranged from 93 to 98 % for all mesh sizes. Since the hydrogel holds some water the water recovery cannot go over 98 %.

Figure 4.1 shows the water recovery percentage for different mesh sizes (55,65,80 and 200 μm) based on different acrylamide monomer concentrations (50,55 and 60 %) in the PAM hydrogel-coated mesh and two concentrations of sodium acrylate in the Na-Ac/AM copolymer. Figures 4.1 A, B and C illustrate the water recovery based on 5, 10 and 30 (v/v) % of original oil content in the mixture, respectively. It is very important to tighten the clamp very well, there are some observations regarding the 200 μm mesh size where it had almost the lowest water recovery compared to other meshes. The poor sealing of the mesh can explain this, as it was thicker and rougher than the other meshes, which led to the possibility of leaking as shown in Figure 3.4. It was observed that with an increase in the monomer concentration from 50 to 60 %, the separation time increases as the hydrogel gets thicker and also most of the samples that are collected do not have visible oil. As the polymer concentration increases, viscosity of the solutions increases as well. It can be seen that the water recovery with the copolymer was less than that of polymer alone due to the higher swelling ability of the copolymer. However, it can seen from Figure 4.1 that water recovery was ranging and fluctuating based on the mesh sizes and monomer concentrations. There

are many possible reasons that can be attributed and some of them are the higher possibility of water getting absorbed by the hydrogel, tightness of sealing, and adhesion force between water and glass tube.

(A)

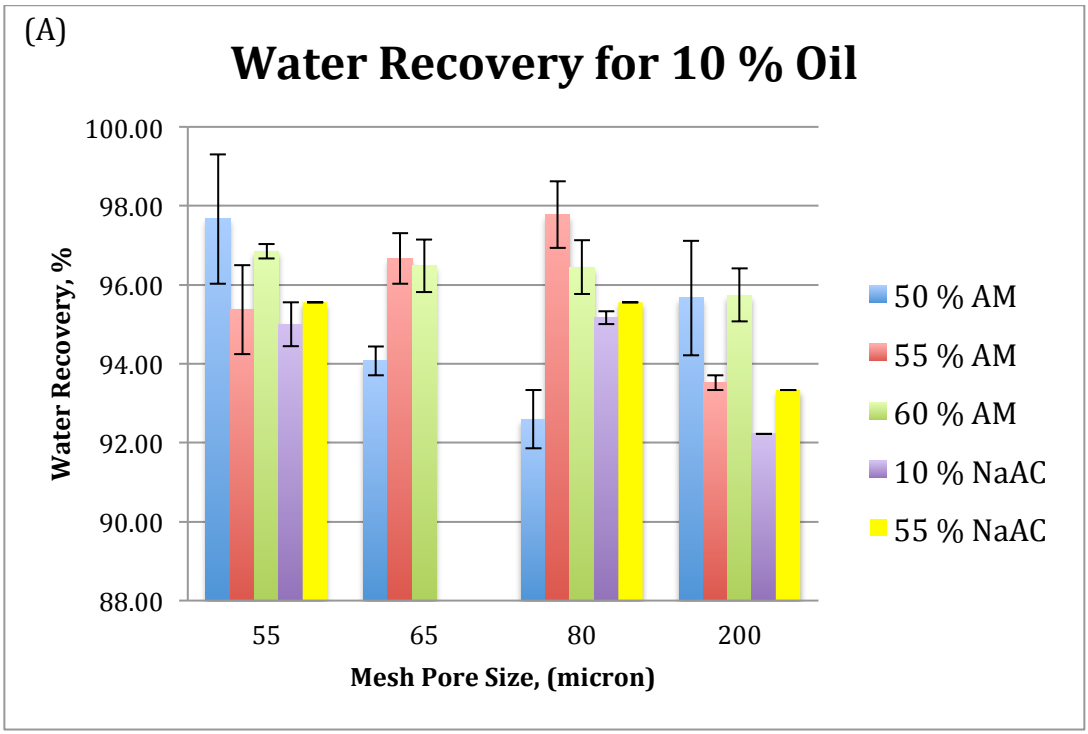

(B)

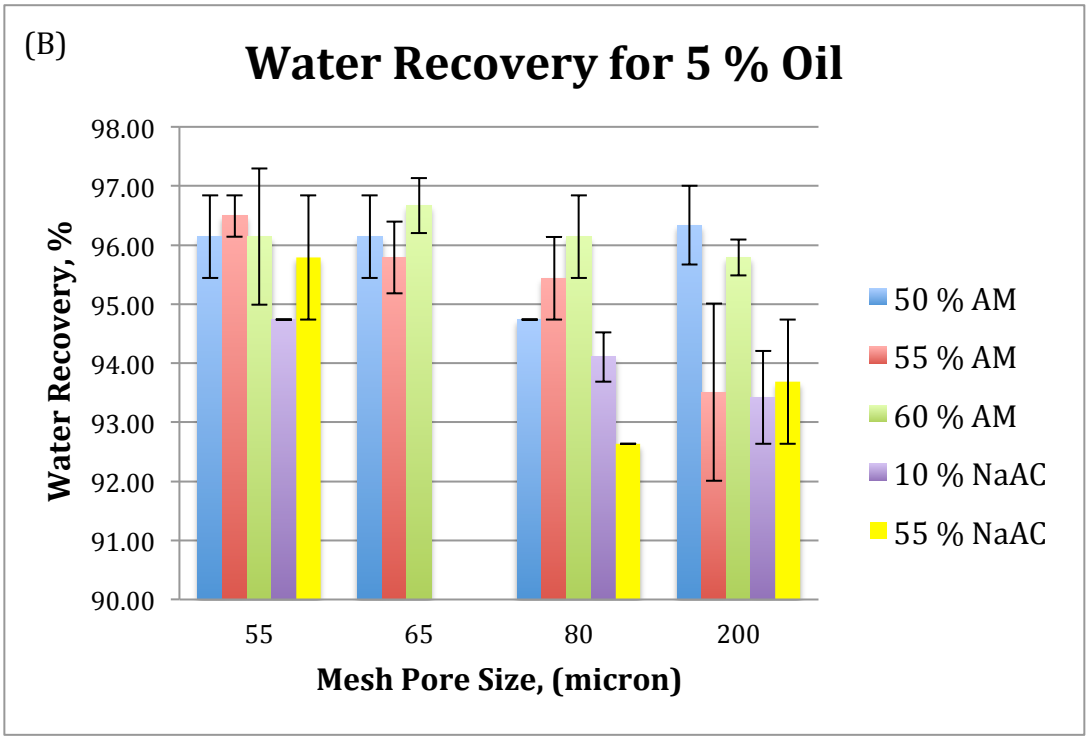

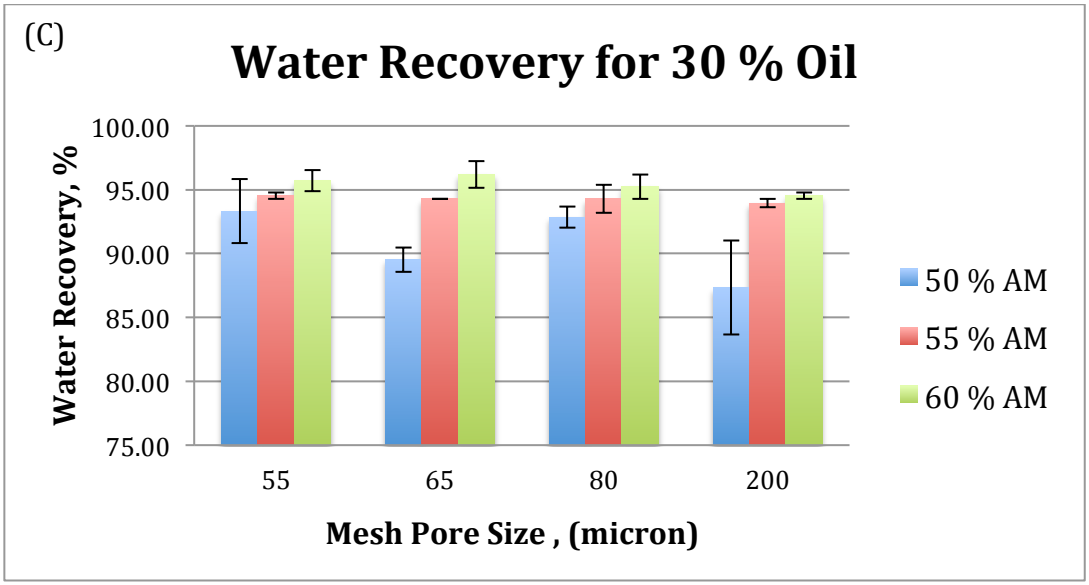

Figure 4.1. Water Recover Percentages of four different mesh (55, 65, 80 and 200 micron) based on 3 different AM concentrations in PAM polymer (50, 55 and 60 wt. %) and 2 different Na-Ac in Na-AC/AM copolymer (10 and 55 wt. %). A, B and C) water recovery based on 5, 10 and 30 % of original oil content in the mixture, respectively. Results are expressed as mean± standard deviation (n=3).

4.1.2 Reclaimed Oil

To confirm the high separation efficiency, the potential presence of residual oil in the filtrated water was measured with UV-visible spectroscopy. Figure 4.2 shows the separation efficiency of PAM and Na-Ac/AM, where A, B and C was for original oil % in water which is 5,10 and 30 % (v/v) respectively. It can be seen that an increase in the oil concentration in water, the separation efficiency decreased. This is an increase in the pressure of oil, which allowed passing of small amount of oil through the pores. Therefore, 30 % oil in water was excluded from the investigation of the copolymer, and moreover larger oil concentration sample are separated using

sedimentation method. Hydrogels were working better with lower oil contents. Reclaimed oil % was determined by measuring the oil percentage in the feed and in the corresponding filtrate (with UV-VIS spectrophotometer) after extraction. The highest separation efficiency of Na-Ac/AM copolymer was for 5 % oil and 10 % NA-Ac in copolymer based on 200-micron mesh was calculated as 93.8 ± 0.24 % in accordance with the value calculated by the volumetric ratio using equation (3.2). Moreover, the separation efficiency of 55 % Na-Ac was lower than 10 % Na-Ac due to the higher amount of sodium acrylate which led to higher swelling index that reduced the hydrogel content from the mesh which can be seen from SEM images. Mainly, separation efficiency dropped with increasing the oil content in water, as there is more pressure on the hydrogel-coated mesh with higher oil content.

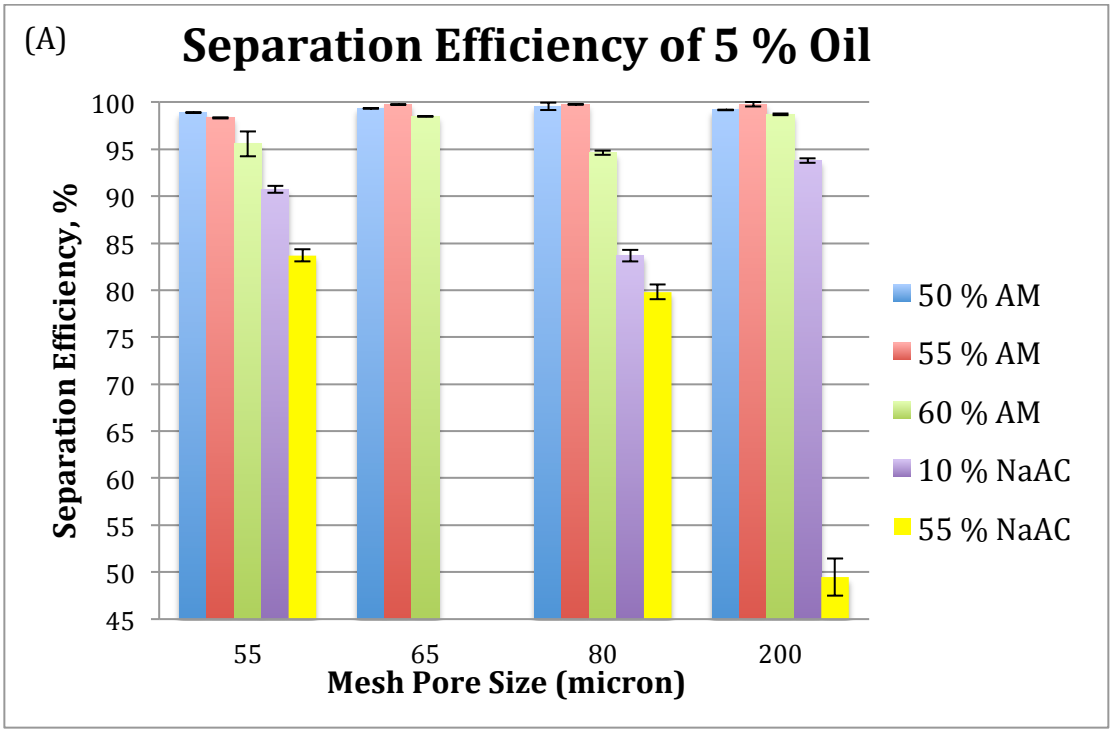

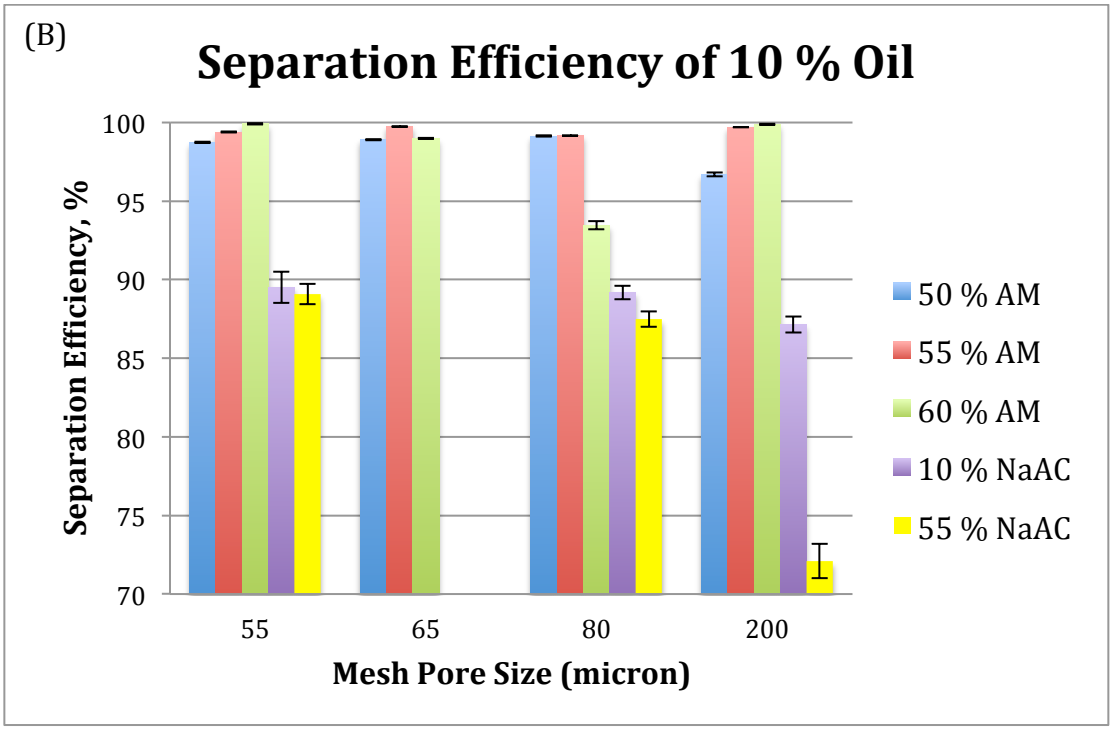

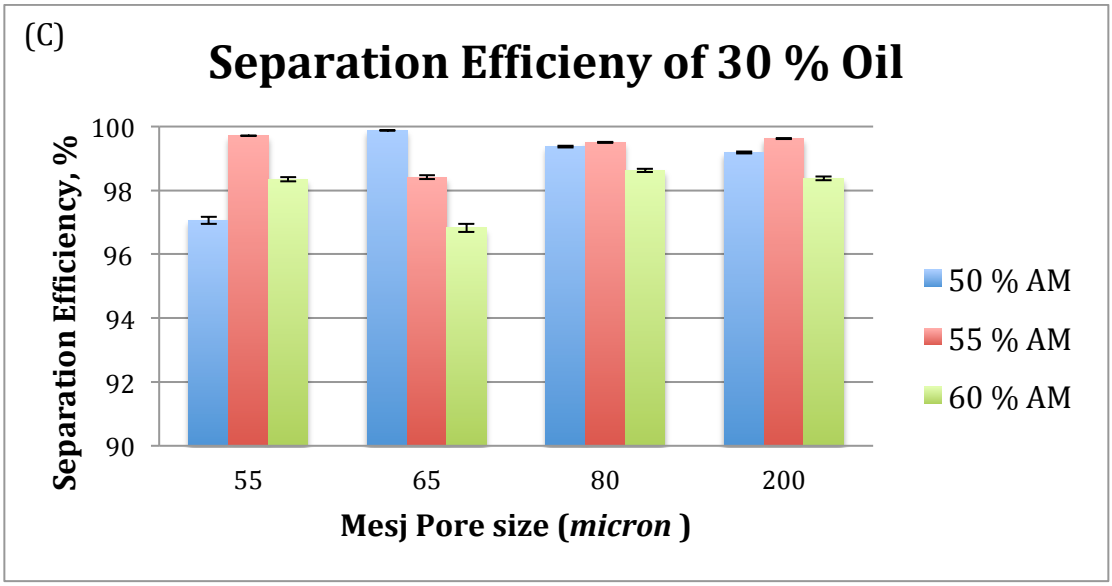

Figure 4.2 Separation Efficiency of PAM polymers and Na-AC/AM copolymer coated mesh based on oil feed content; mesh pore size and monomer concentrations. A, B and C are results for separate oil feed commotions of 5,10 and 30 percentage, respectively. Results are expressed as mean ± standard deviation (n=2).

Due to the super-hydrophilic and the underwater oleo-phobic nature of the PAM coated mesh; water can easily wet and penetrate the treated sample while the oil is

trapped on its surface. Figure 4.3 gives the separation result of 5 % oil from oil/water mixture based on 55 micron size mesh for 55, and 60 % of AM in PAM while Figure 4.4 is for separation of 10 % oil from oil/water mixture based on 55 % AM only in PAM and these samples were chosen as they had separations efficiency with 98.3 and 95.6 and 99.4%, respectively. Also, as shown in the microscopy study of the mixture before and after the separation process, there is a significant difference in the phase composition between the feed and the filtrate, as revealed by the light microscopy images which is evident in Figure 4.3 where the collected filter (right) is transparent compared to the original mixture (left). For oil/water mixture before the separation, densely packed oil droplets flood the entire view (Figure 4.3 (A) and 4.4. (A)), while few tiny droplets are observed in the image of filtrate at all, implying that oil in oil/water has been successfully removed (Figure 4.3 (C, E) and 4.4 (B). It is observed that the feed has much wider droplet size distribution, ranging from 11 to 98 μm with higher frequency, which dropped from 40 to less than 5 and 17 after separation based on 55 and 60 % AM, respectively (Figure 4.3, (B, D and F)). This proved that the separation based on 55 % MA was higher than 60 % AM, and this due to increasing thickness of the hydrogel and higher swelling index which led to cracking in the hydrogel and end up with tiny openings. This indicates the hydrophilicity of the under-water hydrophobic properties of the coated mesh, where water can easily wet and penetrate the coated sample while the oil is trapped on its surface. Microscopic image of filtrated water based on copolymer was not taken as it was done just for PAM to show its higher separation capacity.

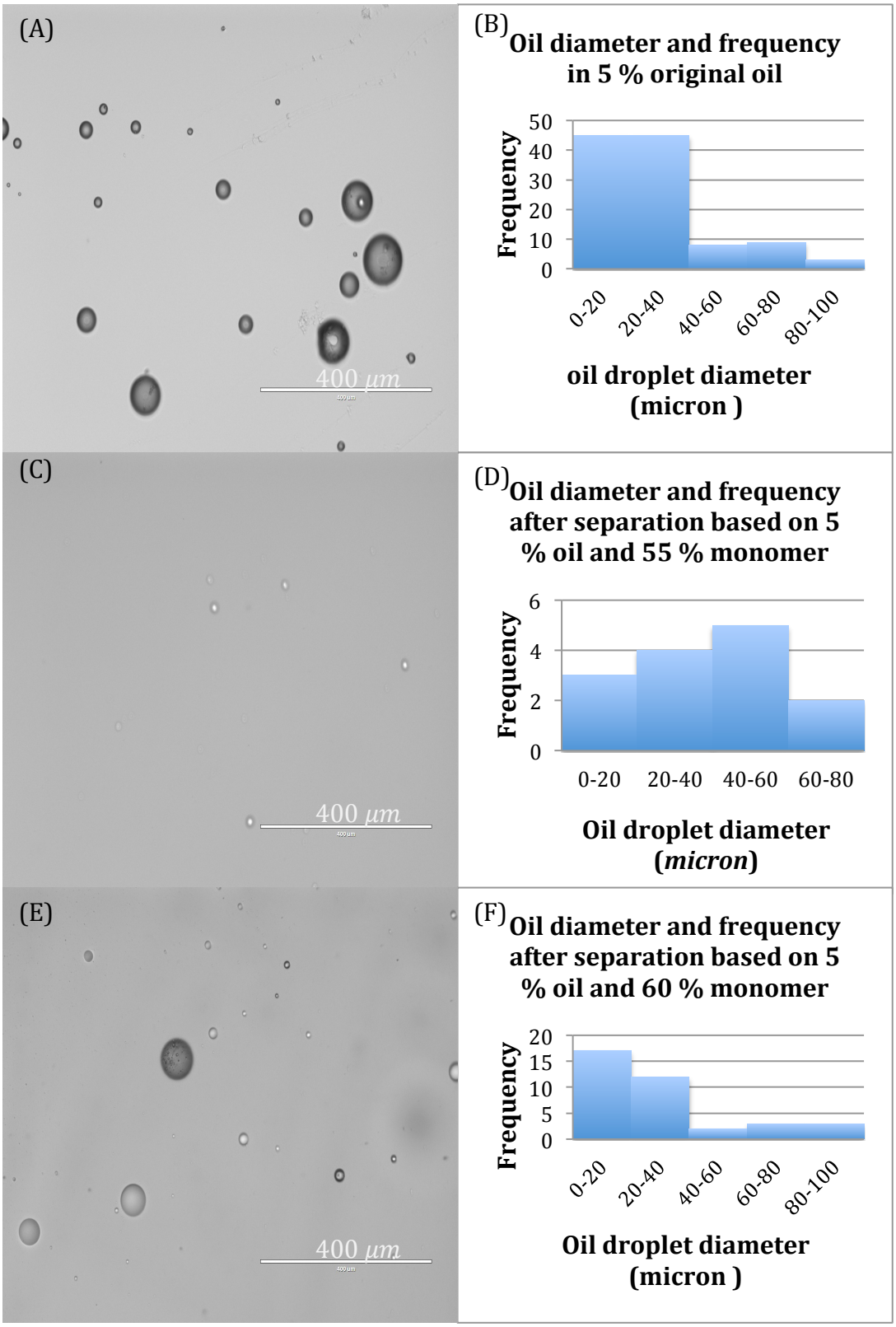

Figure 4.3. Oil/Water microscopic and oil size distribution before and after separation for separation of 5 % original oil from water based on the 55-micron mesh. (A and B)

Microscopic image and oil size distribution for feed composition of 5 % oil. (C-E and D-F) are microscopic images and oil size distribution of filtrated water based on 55 and 60 % AM in PAM, respectively.

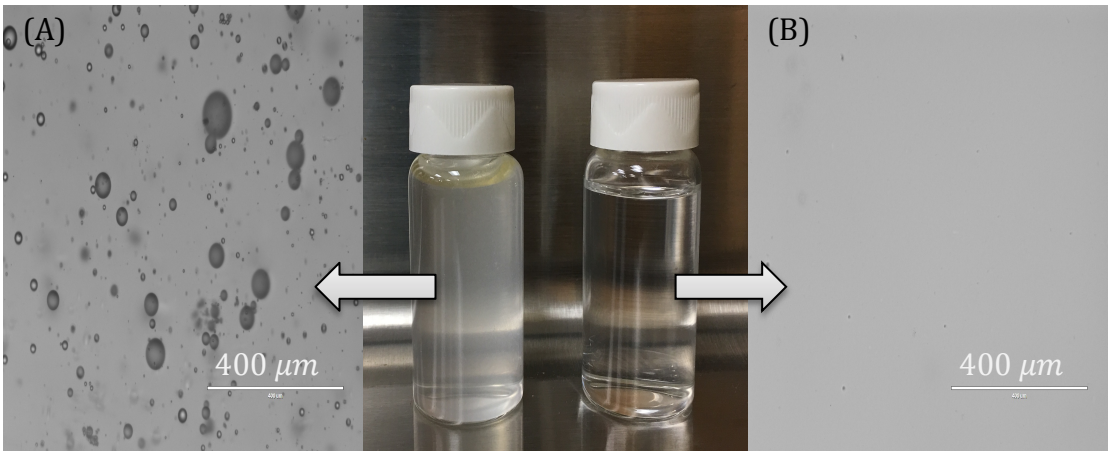

Figure 4.4 Shows (A, B) microscopic and photographic images of 10 % oil before and after separation, respectively. (A) is the 10 % original oil, while (B) is after separation based on the 55 micron mesh and 55 % AM in PAM polymer with 99.4 % separation efficiency, the collected filter (right) is transparent compared to the original mixture (left).

During separation process, the under-water hydrophobicity of PAM coated mesh prevents oil passing through the mesh and prevents the coated mesh from fouling by the oil, and allowing it to be recycled for three times. As PAM hydrogel-coated mesh was used for separation of oil/water mixture, its stability is important factor for practical application. This was investigated by separating oil from water on the same-coated mesh for three times. The separation time decreases with repeatability of using the same coated-mesh, as each batch has six-repeated result three for first separation and another three for the second separation. In the first separation, the coated mesh is highly resistant to oil fouling, but in the second separation, separation time slightly

decrease and oil rejection slightly decrease as shown in Figure 4.5 for 5 % oil based on 55 % AM in PAM with 3 cycles on the same mesh where n=2. The slight decrease is due to the coated hydrogel loss when large amounts of water pass through it. This indicates the PAM hydrogel coated mesh is stable for 3 cycles, however stability of Na-Ac/AM copolymer hydrogel coated mesh could not be determined as hydrogel swollen and pealed off from the mesh after one cycle, which led to lower separation efficiency.

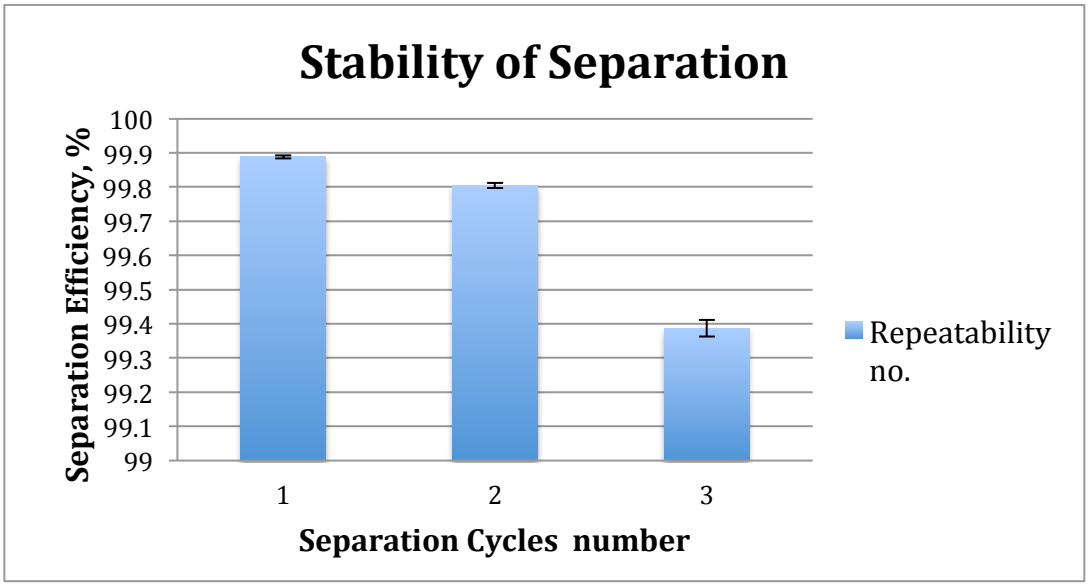

Figure 4.5. Separation stability 5 % oil for PAM hydrogel coated mesh with 55 % AM content 55 micron mesh size. Results are expressed as mean ± standard deviation (n=2).

4.1.3 Separation Time

The effect of pore size of the mesh on the separation time is explained in this section. For a hydrogel coated mesh, it was observed that with an increase in the mesh pores size, the separation time decreased for 55, 65 and 80-micron sizes, while 200

micron mesh has the longest separation time even which has bigger pore size. 50% AM monomer in the PAM hydrogel was the fastest, the reason for this is for lowest monomer content the hydrogel that coated on the mesh is thinner, therefore the separation is faster. However, with increasing the monomer content in the hydrogel, the separation time was longer as the hydrogel getting thicker. It was observed that 60 % AM in PAM polymer was taking longer time for the polymer to dissolve in water around 2 hours and half, however, the separation efficiency is higher than 50 and lower than 55 % AM in PAM. Figure 4.6 (A, B and C) illustrates the separation of time of PAM coated mesh based on oil content on feed compositions for 5,10 and 30 % (v/v), respectively. It shows that separation time was faster with increasing the oil content in water due to the pressure of oil, which affected the separation time. Based on 55 micron mesh, it can been seen from Figure 4.6, separation times for 5 % oil were 1.35, 8.3 and 11 minutes based on 50, 55 and 60 % AM in PAM, respectively, which shows with increasing the acrylamide (monomer) concentration from 50 to 60 %, the separation time increase as we have a thicker hydrogel with less oil content after separation as shown in Figures 4.6 and 4.7.

Though increasing the mesh's pore sizes resulted in the decrease of the separation time, however, the separation efficiency decreased with a negative trend. Again this is an expected result where separation improves with finer mesh size. In conclusion, separation time was increased with increasing the monomer concentration in the polymer as it got thicker and decreased with increasing the oil content in water. However, for investigating the mesh pore sizes, it was found that separation time was decreased from 55 to 80 micron sizes, while it increased for the largest pore size, which was 200 micron. The separation time for the four different mesh sizes and three

monomer concentrations were less than 30, 25 and 8 minutes based on 5, 10 and 30 oil %, respectively.

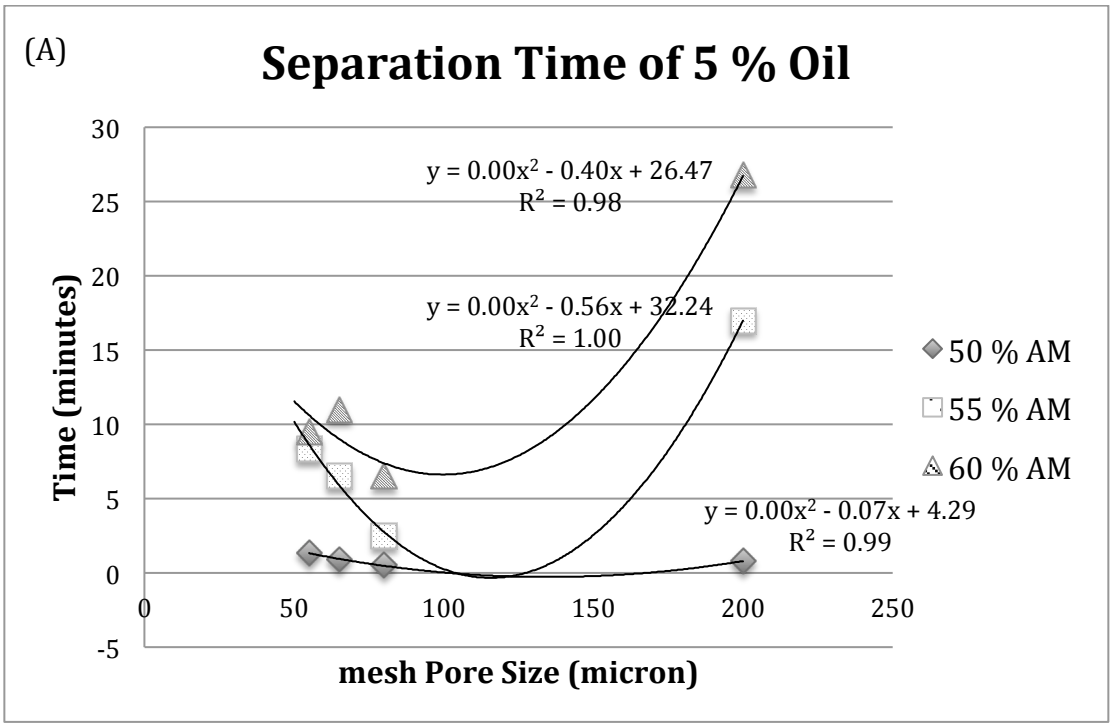

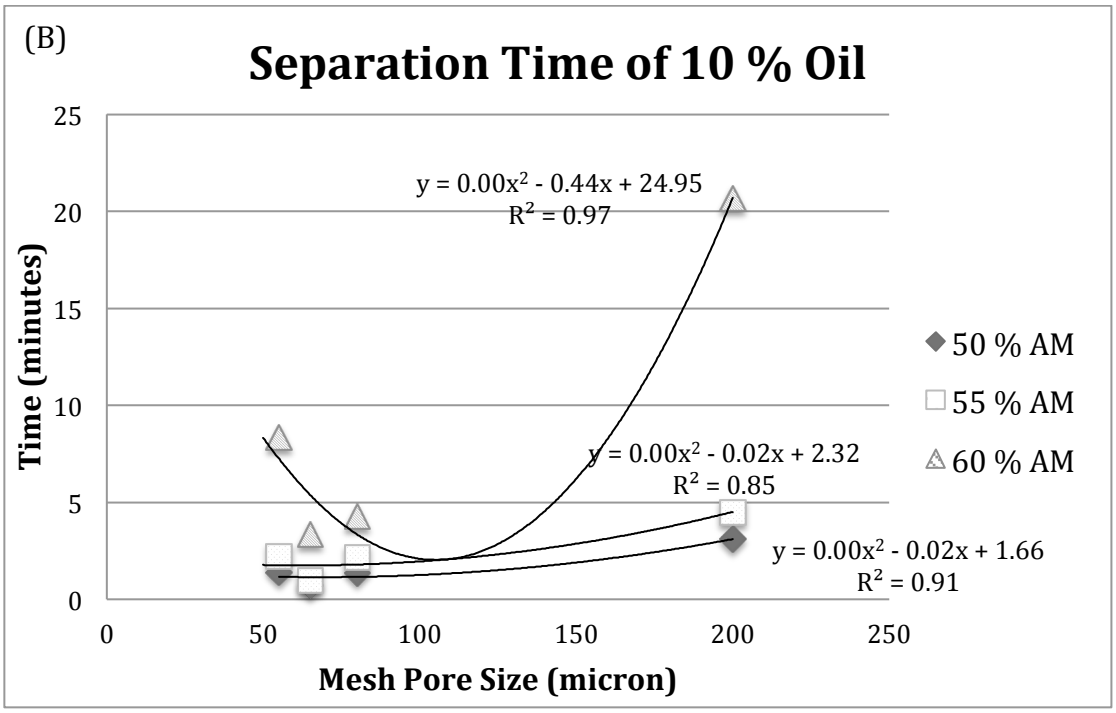

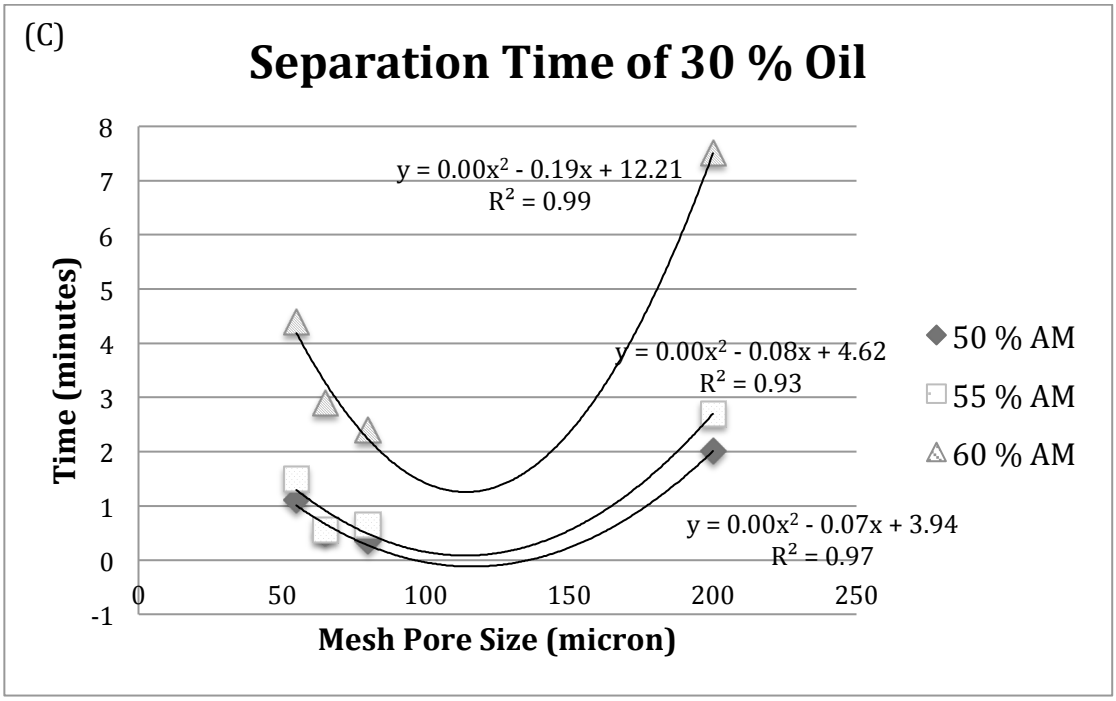

Figure 4.6. Separation time of oil/water mixture for PAM hydrogel coated mesh with three different acrylamide concentrations in the PAM, which are 50,55 and 60 %, based on 55,65,80 and 200 micron meshes. A, B and C) separation time base d on oil feed compositions 5, 10 and 30, respectively. Results are expressed as mean ± standard deviation (n=3).

In contrast, Figure 4.7 indicates separation time of oil/water mixture for Na-Ac/AM copolymer hydrogel with two different Na-Ac concentrations in the copolymer which are 10 and 55 % for three different mesh sizes which are 55, 80 and 200 micron mesh based on 5 and 10 oil % in A and B, respectively. Separation time of Na-Ac/AM copolymer was faster than the PAM polymer; this is due to a higher swelling ratio of copolymer as it swells very fast than the polymer due to the ionic charges in sodium acrylate. Moreover, 55 % of Na-Ac was faster than 10 % due the swelling and higher content of sodium acrylate. In addition, the separation time was less than 70 second and this is going to be explained later in section 4.5. It must be mentioned that 200 micron coated mesh with 10 % Na-Ac had the higher separation

efficiency with 93.8 % and this is due to the higher percentage of acrylamide (45 %) which has ability to reject and prevent oil from penetrating through it.

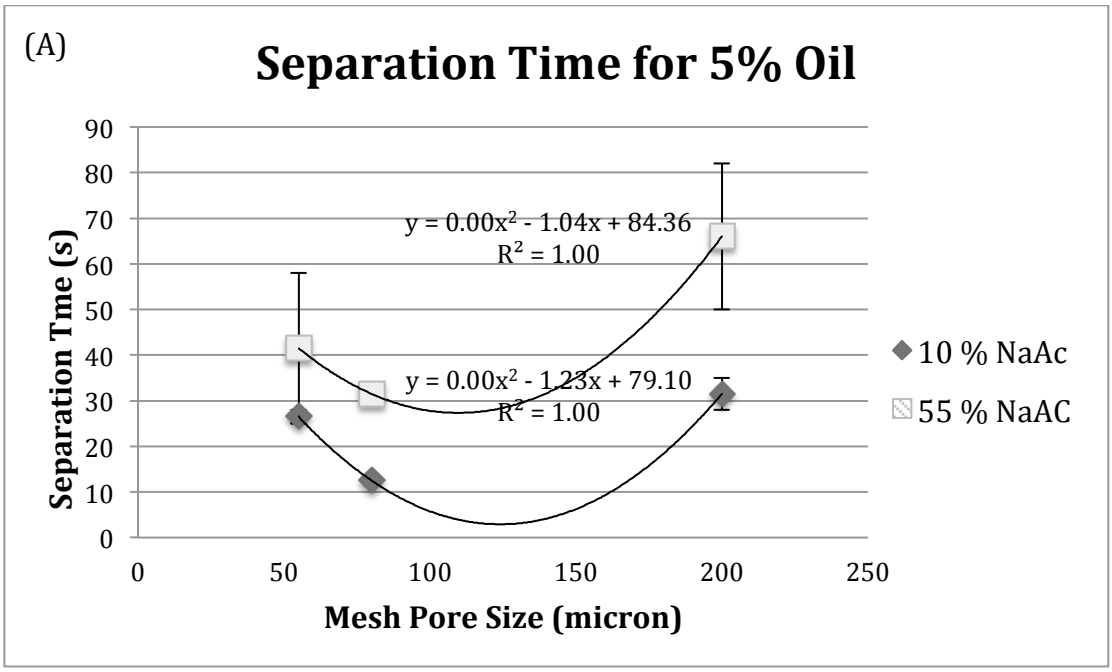

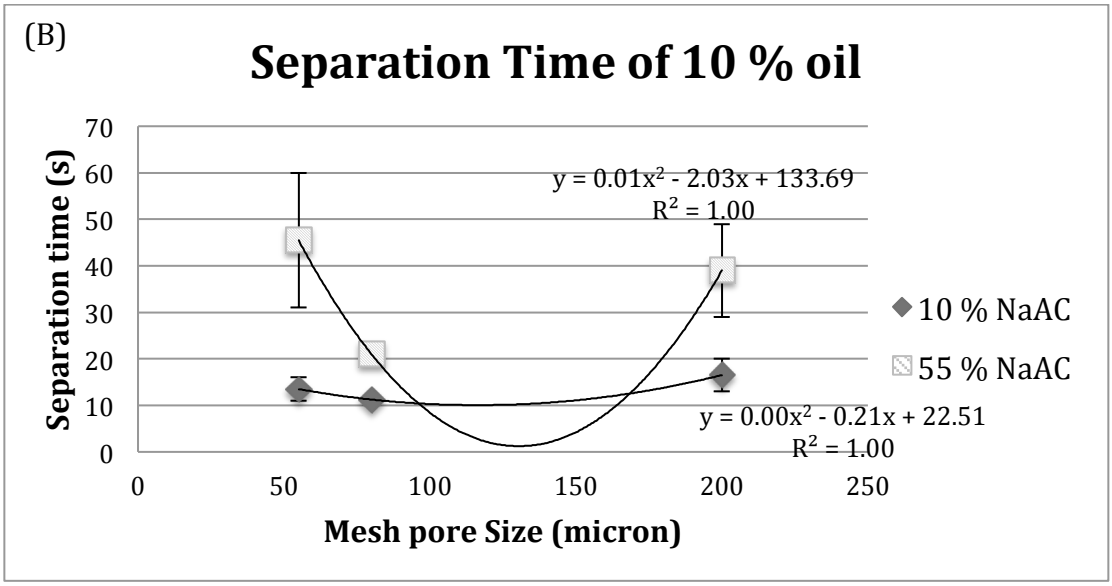

Figure 4.7. Separation time of oil/water mixture for Na-Ac/AM copolymer hydrogel with two different Na-Ac concentrations in the copolymer which are 10 and 55 % for three different mesh sizes which are 55, 80 and 200 micron mesh. Results are expressed as mean ± standard deviation (n=3).

4.2 Wettability

It is well known that the wettability of the solid surface mainly depends on both the geometrical structure (roughness) of the surface and the chemical compositions.[12,53] The performance of the coated mesh is remarkable with extreme difference in the oil and the water contact angle. If underwater OCA is greater than OCA in air or greater than 150 degree, this will indicate the underwater super hydrophobic of hydrogel-coated mesh. This phenomenon is occurs due to the formation of water cushion between the solid surface of the PAM hydrogel coated mesh which is composed of water molecules in the rough surface and the oil droplet, which create a strong repulsive force due to interaction between the oil (non-polar) and the water (polar) molecules[10,12,53]

In air, water-wetting behavior on the PAM coated mesh was improved compared to the original uncoated mesh, which had a water CA of less than 5°. As shown in Figure 4.8, when water droplet (5 μl) contacted with the surface of PAM (55 micron) coated mesh, it quickly spreaded and penetrated through the mesh with CA $<5^{\circ}$ above the mesh and water could easily drip down, when more water droplets were added on the surface of the coated mesh, which indicates a good hydrophilicity and permeability of the coated mesh to water. Figure 4.9 shows the difference between water and oil droplet's shape in air on PAM coated mesh of 200-micron size. Water droplet was spread and permeated on the coated mesh, which was absorbed very fast in (Figure 4.9 (A)), while in (B) oil droplet was spread on the coated mesh with around 15 degree due to the viscosity of oil. Water contact angles on PAM hydrogel coated mesh, were hard to measure in air, as it penetrated very fast. Therefore, PAM hydrogel coated mesh is super-hydrophilic in an air-solid-liquid the three phase

system with both oil contact angle (OCA) and water contact angle (CA) lower than 10°.

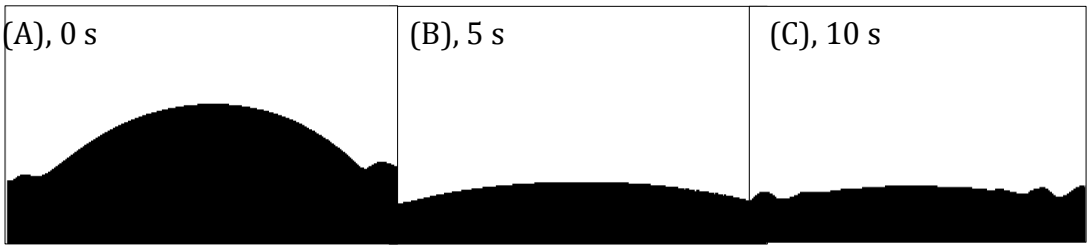

Figure 4.8. Water wettability of PAM hydrogel- coated mesh and spreading and permeating of water droplet ($5\mu l$). (A, B) water quickly permeates and spreads through the coated mesh (55 micron) within 2 seconds, (C) droplet decreases from 16.29 to <5 degree within, where absorbed 10 second.

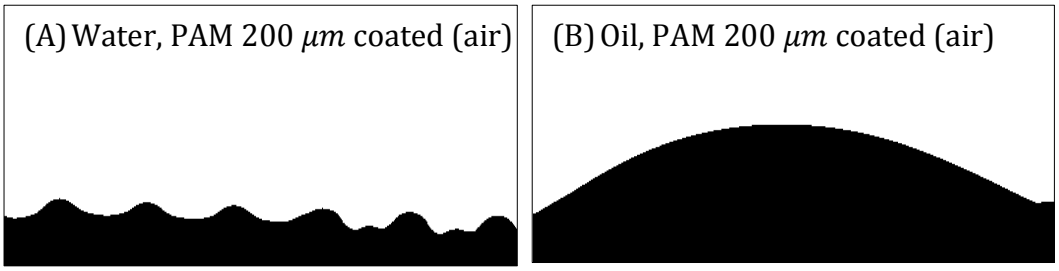

Figure 4.9. CA & OCA based on 200 micron mesh in air. (A& B) PAM coated-mesh. A) Spreading and permeating Water droplet on the coated mesh which was absorbed very fast; B) Oil droplet spread on the coated mesh with 15 degree.

From Figures 4.10, without the coating, the original stainless mesh exhibited oleo-phobic properties up to 100° of water CA that is greater than the water CA of coated mesh due to the hydrophobicity of the stainless steel mesh, which form a sphere. Moreover, with increasing the pore size, water CA increased on the uncoated mesh

due to air trapped between the pores and getting higher contact angle as shown in Figure (4.10).

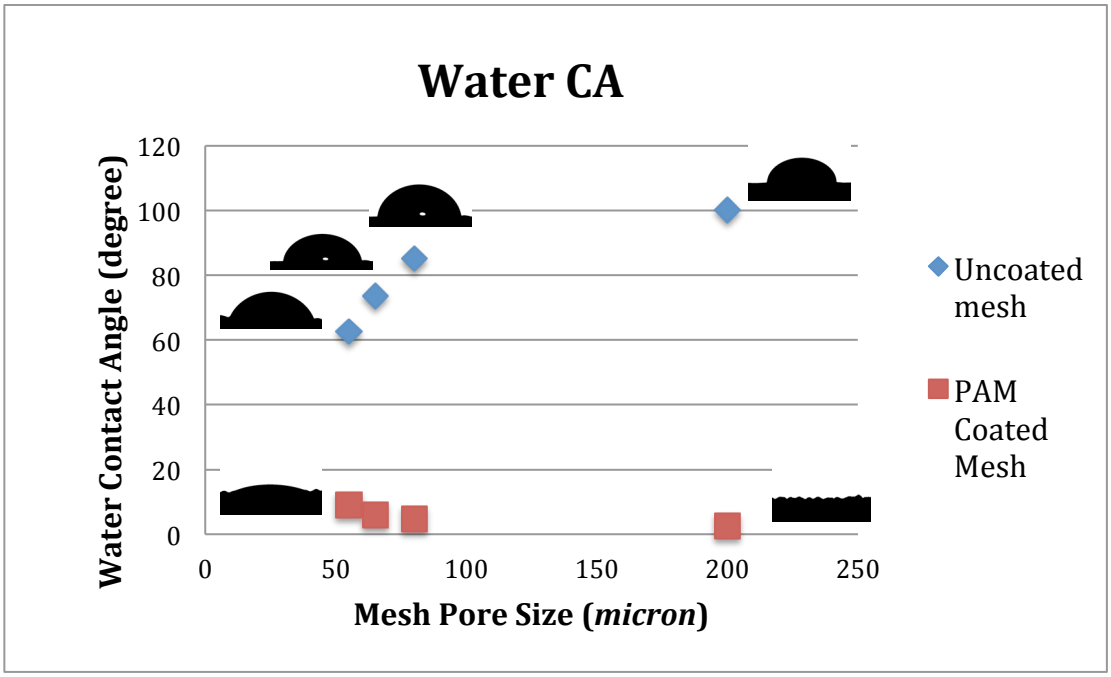

Figure 4.10. CA & OCA of uncoated and PAM coated meshes with four different pore sizes, (55,65, 80 and 200 micron). Results are expressed as mean ± standard deviation (n=4).

Various polymer coating can be designed by using the original meshes with different pore sizes as the substrates. Figure 4.11 describes the relationship between the pore diameter of the meshes and the under-water OCAs on the coating mesh with 3 different monomers. Within the experimental error, the OCAs for 55 micron mesh based on 60 % AM in PAM was 140.03 ± 0.88 ° .For 65 micron mesh it is 117.9 ± 1.5 ° after which it increases gradually with increasing pore size of the mesh. On the other hand, the water CAs on all the coated meshes was less than 5°. These results indicate that the hydrophobicity of the coating mesh is affected by the size of the pores and roughness of the surface. If the roughness of the membrane increases, then the contact area between the membrane and the oil decreases.

Under-water, when the coated mesh contacts with the oil droplet, more water can be trapped in the rough microstructure, forming an oil/water/ solid composite interface. These trapped water molecules will also reduce the contact area between the oil and the coated mesh, resulting in a large oil CA under-water, which leads to a dramatic increase in oleophobicity. For 60 % acrylamide in the hydrogel, all the OCAs are greater than 115 degree and up to 140° (Figure 4.11). According to the literature, the adhesion forces for different oils such as gasoline, vegetable oil, crude oil diesel, hexane and other petroleum is less than 5 μN on PAM hydrogel coated mesh, which proves that low adhesion properties can prevent PAM coated mesh from fouling by oil during the separation process.[10,24,52]

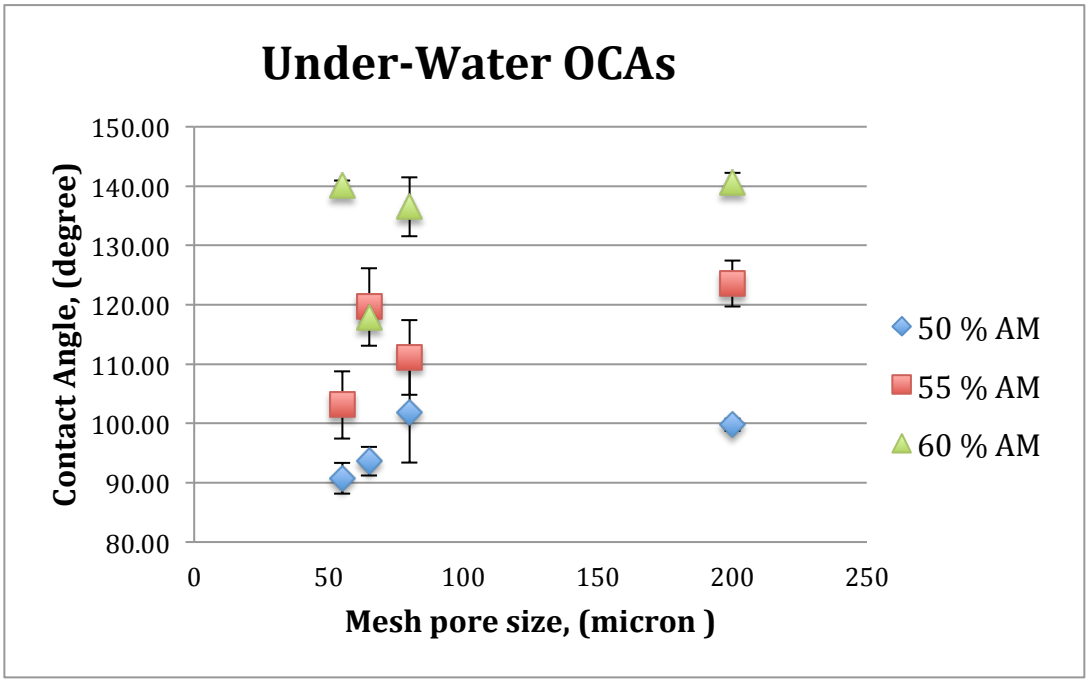

Figure 4.11. Under-water OCA and the relationship between the oil contact angles (1,2-dichloroethane) and the pore diameters of PAM hydrogel-coated mesh based on

three different monomer concentrations. Results are expressed as mean ± standard deviation (n=4).

Figure 4.12 shows the wetting behaviour of 1,2-dichloromethane (DCE) on the PAM coated mesh with different monomer concentrations and mesh sizes. It can be seen that under-water OCA increases with increase in the monomer concentrations in the hydrogel due to a decreasing contact area between the coated mesh and the oil droplet (DCE). This is in agreement with the fact that the wettability of the surface is mainly governed by the roughness and its chemical compositions.[10,27,30]

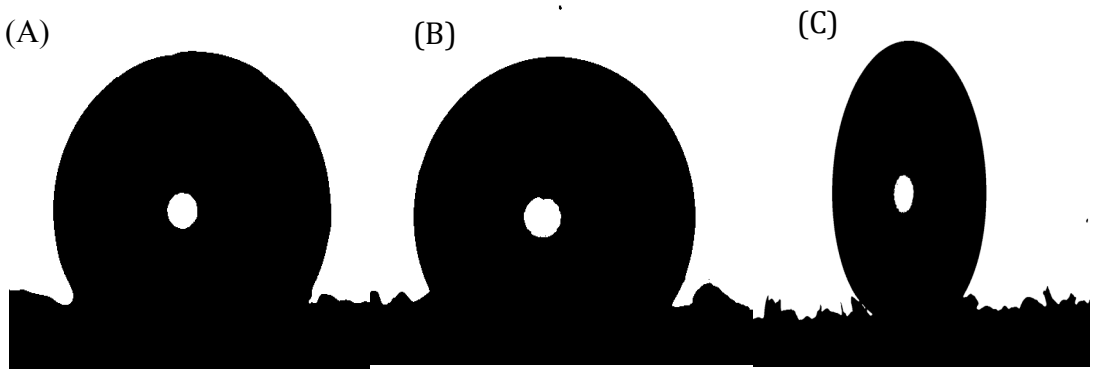

Figure 4.12. Photographs of under-water OCA (DCE, 5 μ L) on 55 micron mesh based on three different monomer concentrations in the PAM hydrogel, A) Shape of the OCA on the coated mesh with ($90.7 \pm 2.56^{\circ}$) for 50 % AM, B) OCA with ($103.11 \pm 5.7^{\circ}$) for 55 % AM. C) OCA with ($140.03 \pm 0.87^{\circ}$) for 60 %AM.

Wettability of AM/Na-Ac copolymer coated mesh could not be investigated by measuring oil contact angles under-water. It was very hard as the copolymer swells very fast and pealed off from the mesh, which ended up with difficultly with the measurements.

4.3 Hydrogel Coating Percentage (HCP)

The percentage of the hydrogel-coated mesh was determined based on different mesh pore sizes (55,65,80 and 200 micron) for different monomer concentration (50,55 and 60%) and calculated using equation (3.4).

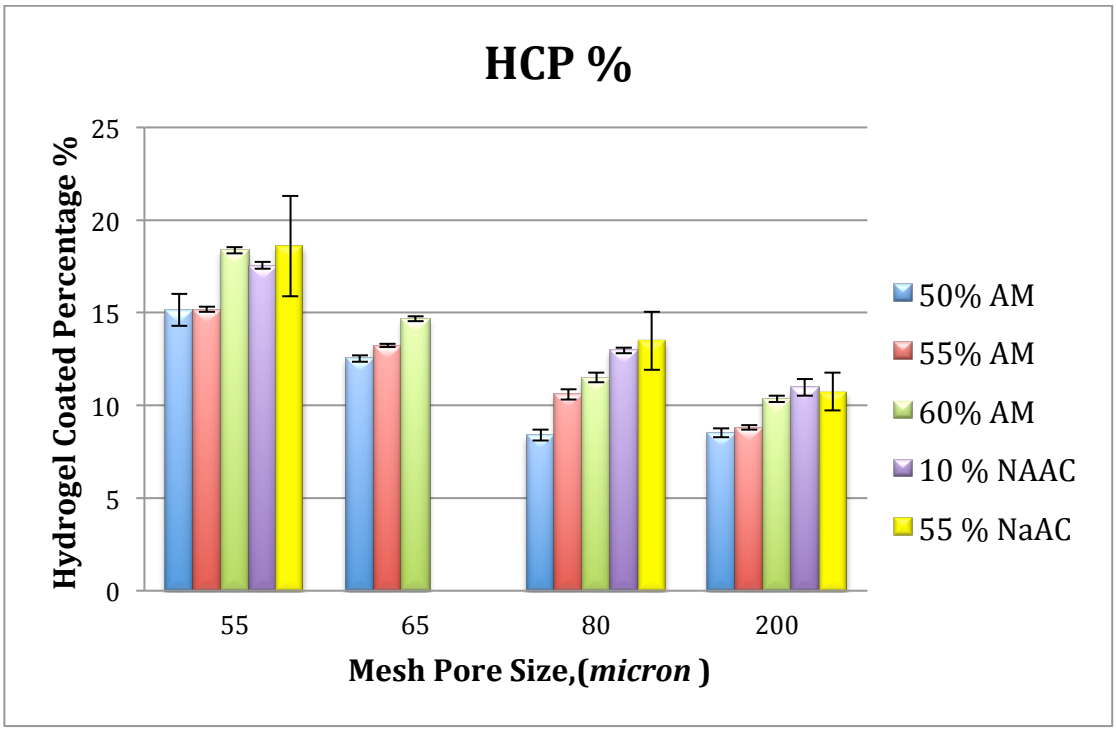

Figure 4.13. Hydrogel Coated Percentage (HCP) of PAM hydrogel as a function of meshes sizes based on 50,55 and 60 wt. % on monomer, and HCP for Na-Ac/AM copolymer as a function of mesh sizes based on 10 and 55 wt. % of the Na-Ac co-monomer. The value obtained by determining the increased weight percentage of the mesh after polymerization. Results are expressed as mean ± standard deviation (n=4).

It indicates that from Figure 4.13, the smallest mesh pore size was coated with gel more than the coarse mesh, which improved the absorbing ability of the hydrogel, which enhances the oil/water separation. Moreover, increasing the hydrogel

concentration increases the percentages hydrogel-coated on the mesh. With low monomer content, the hydrogel was thinner than with a higher monomer concentration, and the separation time is faster but separation efficiency is less than that of thicker hydrogel. This was confirmed with HCP measurements, which proved that hydrogel gets thicker with increasing total monomer concentration.

4.4 The Swelling Index

Swelling Index was calculated to quantify the hydrogel ability to absorb water by using equation 3.3. The swollen hydrogels were removed from water after 5, 10, 20, and 1440 and 2880 minutes, excess water was wiped with filter paper and then weight quickly. Hence a dried hydrogel (dry gel) can absorb a large amount of water. Four samples were taken for each experiment, and the reported data points represent the averages of the four data points. Figure 4.14 shows that the swelling index of all monomer concentration increases gradually within one day, but it decreases by 3 % for 50 and 60 % AM and by 6% for 55 % AM after 48 hours. Figure 4.15 indicates the swelling of PAM hydrogel (55 % AM) within two Days, A) when the dry hydrogel just left in water for 5 seconds, B, in 5 minutes with 104.08 ± 9.93, C and D within 10 and 20 minutes with 118.18 ± 14.22 and 137.44 ± 14.22, respectively and E and F are the swollen hydrogel within 24 and 48 hours which had swollen degree of 167.35 ± 8.32 and 161.15 ± 8.8 %, respectively.

The swelling of the hydrogel is induced by the electronic repulsion of the ionic charges of its network. [34] The ionic charge content has a strong effect on the swelling. Sodium acrylate has many ionic units (-COONa), therefore, the swelling increases due to increasing anionic units.[54] The salt group is almost ionized, and a large number

of hydrophilic groups appear. The hydrophilic group of AM/Na-Ac copolymers are higher than those of acrylamide, thus the swelling of AM/Na-Ac copolymers is greater than the swelling of PAM polymers. The 10 and 55 % Na-Ac copolymers swell rapidly, and its swelling ratio was 272.15 ± 0.29 and 329.51 ± 6.28 % within 24 hours, respectively; and the copolymer swelling reduced by 4 and 15 % after 48 hours, respectively (Figure 4.14). Figure 4.16 illustrates dry hydrogel of 10 % Na-Ac (A) and swollen hydrogel after 48 hours with 268.23 % of swelling index (B). It can be concluded that adding small amount of Na-Ac monomer to PAM is going to enhance and increase swelling ratio and its ability to absorb water. While Figure 4.17 indicates the photograph images of swelling of Na-Ac/AM copolymer hydrogel with 55 % of sodium acrylate within two Days, A is the dry hydrogel when just left in water for 5 seconds, B, C and D are the swollen hydrogels after 5, 10 and 20 minutes with swelling index of $172.45 \pm 18.63, 244.5 \pm 10.26$ and 297.09 ± 10.05, respectively, while E and F are the swollen hydrogel within 24 and 48 hours at 329.51 ± 6.28 and 313.56 ± 6.72, respectively. In conclusion, as the concentration of the monomer increases the swelling capacity of the copolymer increases up to a certain level, but within two days the swelling capacity decreases drastically.

The crosslinking concentration was 1.5 % in PAM and the copolymer and was maintained constant. From the classical behavior of hydrogels, swelling ratio decreases with an increase in the crosslinking concentrations. This is due to the fact that the distance between the crosslink is smaller when the crosslinking amount increases, which inturn restricts its swelling capacity. [38]

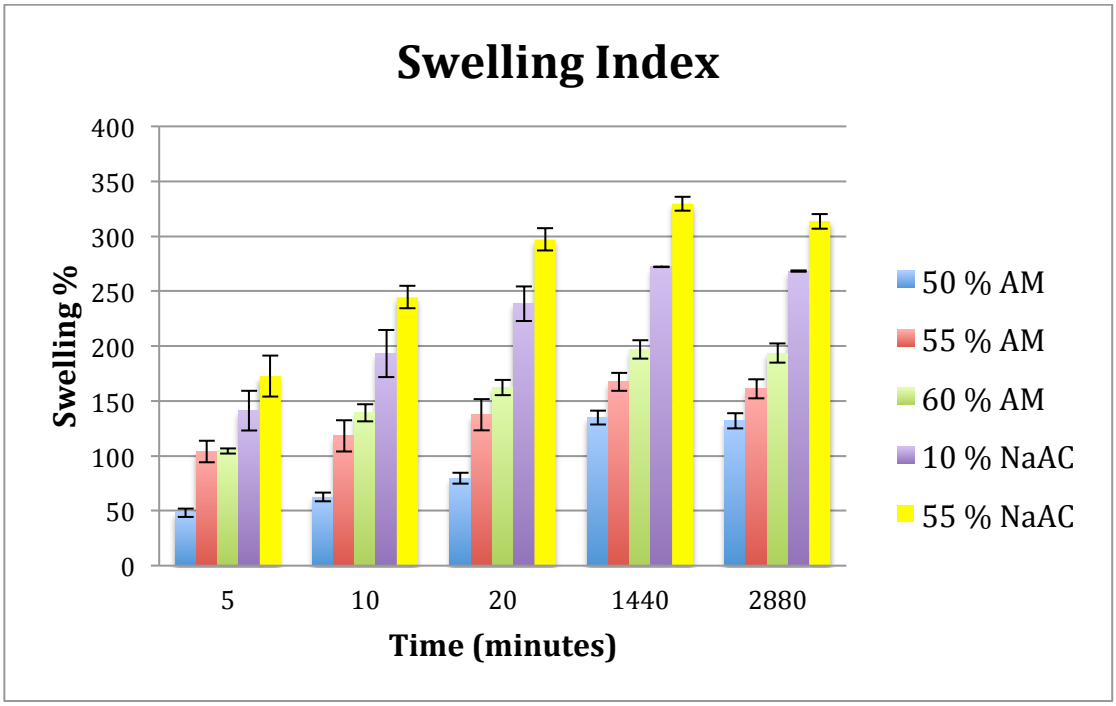

Figure 4.14. Illustrates Swelling Index of 50, 55 and 60 % monomer in PAM hydrogel, and 10 and 55 % Na-Ac in the copolymer. Results are expressed as mean ± standard deviation (n=4).

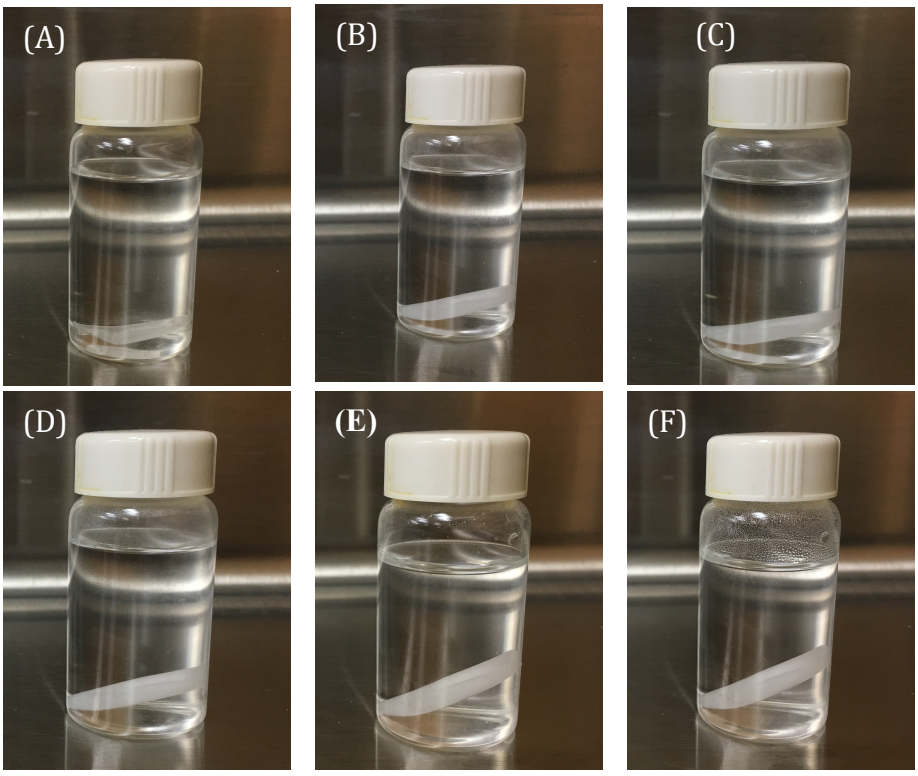

Figure 4.15. Photograph of swelling PAM hydrogel (55 % AM) within two Days. A) When dry hydrogel just left in water for 5 seconds. B, C and D) are swollen hydrogel after 5, 10 and 20 minutes, respectively. E and F are the swollen hydrogel within 24 and 48 hours, respectively, which swell 161.15 $\pm$ 8.8 % within two days.

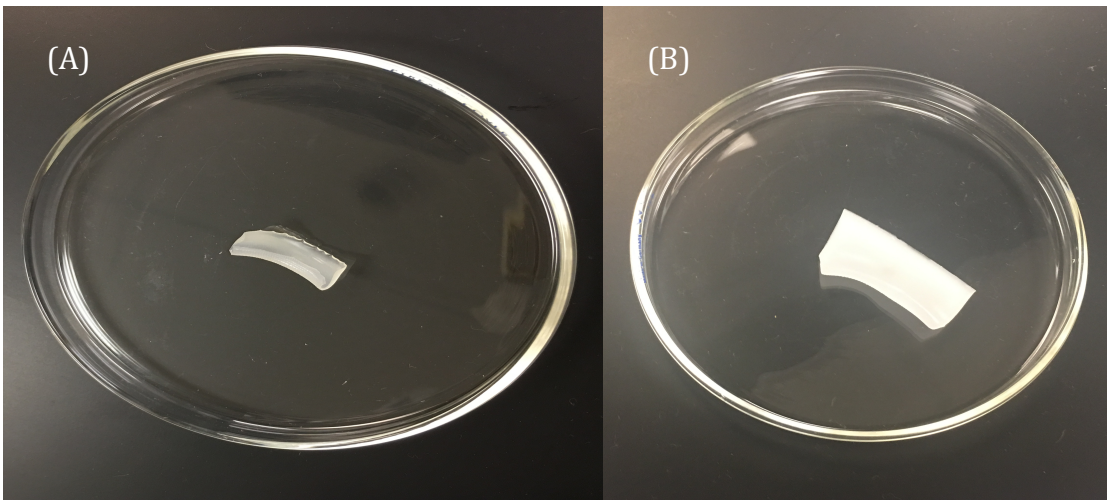

Figure 4.16. Illustrates dry Na-Ac/AM copolymer (10 % Na-Ac) hydrogel in (A) and swollen hydrogel after 48 hours with 250 % of swelling index in (B).

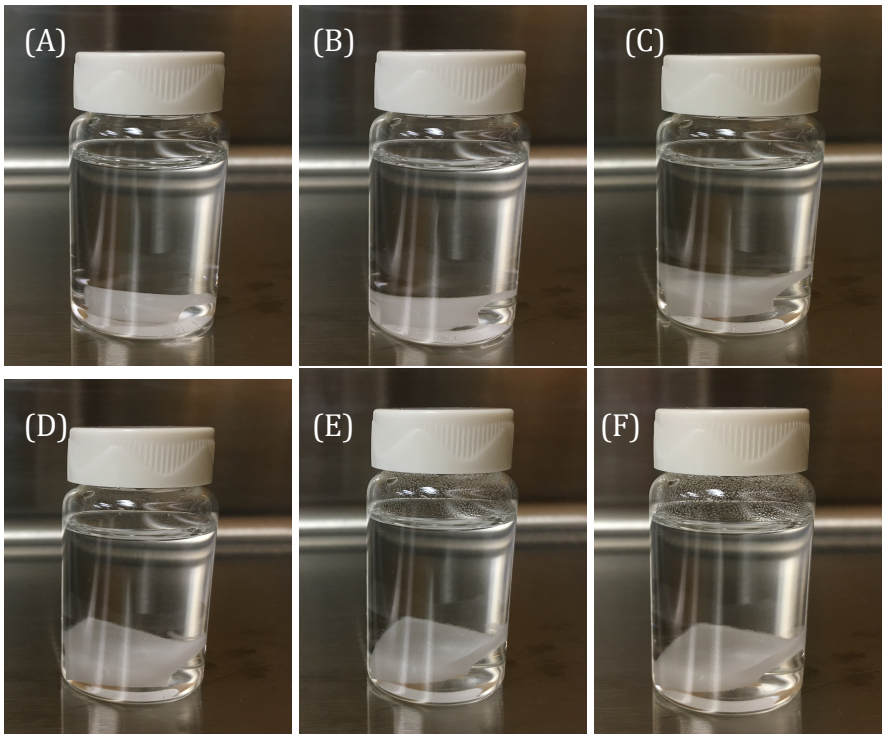

Figure 4.17. Images of swelling of Na-Ac/AM copolymer hydrogel (55 % Na-Ac) within two Days. A) Dry hydrogel when left in water for 5 seconds. (B, C and D) are the swollen hydrogels after 5, 10 and 20 minutes, respectively. (E and F) are the swollen hydrogel within 24 and 48 hours, respectively.

4.5 Scanning Electron Microscopy (SEM)

Scanning electron microscopy measurements were carried out to characterize the surface morphologies of the mesh before and after coating. Figure 4.13 shows the SEM images of PAM polymer (60 %AM) coating mesh made from a stainless steel mesh with a pore diameter of about 200 and 55 micron. Typical images of the uncoated mesh substrates that are waves stainless steel with pores diameter of 55 and 200 microns is shown in (E and A), respectively, which indicates the original meshes have a smooth and clear surface. The micro-porosity of the coated mesh can be controlled by different mesh sizes and hydrogel contents. It is clear from the SEM images in Figure 4.18 that the surface of the PAM hydrogel was less rough and smother than the mesh with Na-Ac/AM copolymer, which was swollen, and pealing off. It can be seen that a rough coating is formed on the stainless steel mesh and mainly exists between the pores, which ensures that there is no free opening through which oil can pass through it. The coating distributes uniformly and the porous structure is mostly retained in the prepared mesh. More hydrogel exists in the pores of the mesh, which ensures blocking of the open area with smaller free passage for water passing through the coated mesh.[23] The reason for hydrogel being between the grids more than on the wires, is due to the structure of the stainless steel meshes which are wire woven without aside open pore due to smaller it's size (in microns). The reinforcement method for mesh is used to support the hydrogel during graft polymerization.

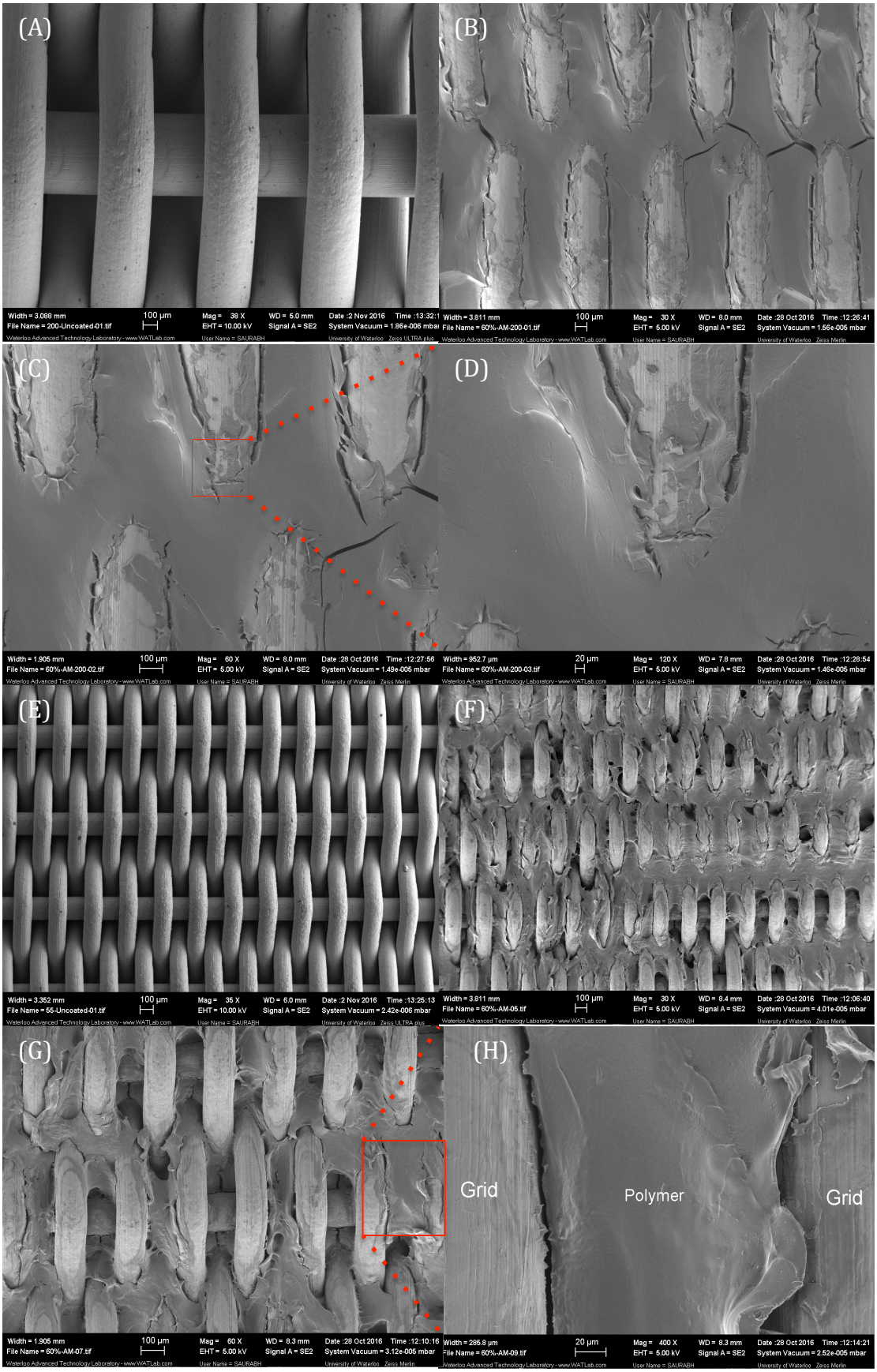
(A)
Width = 3.088 mm
File Name = 200-Uncoated-01.tif
100 µm
Mag = 38 X
EHT = 10.00 kV
WD = 6.0 mm
Signal A = SE2
Date :2 Nov 2016 Time :13:32:1
System Vacuum = 1.86e-006 mbar
(B)
Width = 3.811 mm
File Name = 60%-AM-200-01.tif
100 µm
Mag = 30 X
EHT = 5.00 kV
WD = 8.0 mm
Signal A = SE2
Date :28 Oct 2016 Time :12:26:41
System Vacuum = 1.56e-006 mbar
(C)
Width = 1.905 mm
File Name = 60%-AM-200-02.tif
100 µm
Mag = 60 X
EHT = 5.00 kV
WD = 8.0 mm
Signal A = SE2
Date :28 Oct 2016 Time :12:27:56
System Vacuum = 1.49e-006 mbar
(D)
Width = 952.7 µm
File Name = 60%-AM-200-03.tif
20 µm
Mag = 120 X
EHT = 5.00 kV
WD = 7.8 mm
Signal A = SE2
Date :28 Oct 2016 Time :12:28:54
System Vacuum = 1.46e-006 mbar
(E)
Width = 3.362 mm
File Name = 55-Uncoated-01.tif
100 µm
Mag = 35 X
EHT = 10.00 kV
WD = 6.0 mm
Signal A = SE2
Date :2 Nov 2016 Time :13:25:13
System Vacuum = 2.42e-006 mbar
(F)
Width = 3.811 mm
File Name = 60%-AM-05.tif
100 µm
Mag = 30 X
EHT = 5.00 kV
WD = 8.4 mm
Signal A = SE2
Date :28 Oct 2016 Time :12:06:40
System Vacuum = 4.01e-006 mbar
(G)
Width = 1.905 mm
File Name = 60%-AM-07.tif
100 µm
Mag = 60 X
EHT = 5.00 kV
WD = 8.3 mm
Signal A = SE2
Date :28 Oct 2016 Time :12:10:16
System Vacuum = 3.12e-006 mbar
(H)
Grid
Polymer
Grid
Width = 286.8 µm
File Name = 60%-AM-09.tif
20 µm
Mag = 400 X
EHT = 5.00 kV
WD = 8.3 mm
Signal A = SE2
Date :28 Oct 2016 Time :12:14:21
System Vacuum = 2.52e-006 mbar

Figure 4.18 SEM images of PAM polymer (60 %AM) coating mesh prepared from a stainless steel mesh with a pore diameter of about 200 and 55 micron. A) Un-coated 200 micron original mesh, Band C) large and enlarge view area of the PAM coating mesh on 200 micron with 10 μm scale bar in C; D) is uncoated 55 micron mesh; E and F) large and enlarged view of the PAM coating mesh on 55 micron mesh; G) higher-magnification image of PAM hydrogel coated between the grid of 55 micron mesh.

Figure 4.19 shows the scanning electron microscopy (SEM) image of a large area of copolymer coating mesh (10 and 55 % Na-AC) with pore size diameter of 55 and 200 micron. Scanning electron images show large aggregation in the copolymer hydrogel with higher sodium acrylate, which held together by intermolecular hydrophobic association to form a 3D network and these is due to the high viscosity of the copolymer, which was also reported by Zhang Bin.[55,56] Therefore, large aggregation shows strong intermolecular interaction and high swelling rate, where hydrogel was getting off the mesh which end up with open areas that tiny oil can pass through them. Hydrophobicity is improved with surface roughness because air can be trapped between the solid surface and the droplet, which led to minimizing the contact area. Figure 4.19 B and D show the copolymer hydrogel with 10 % Na-AC which was more smother and coating uniformly on the mesh, while F and H were higher magnification image of 55 % Na-AC copolymer with more roughness and swelling due to the higher content of sodium acrylate and this mesh with 200 micron had the lowest separation efficiency at 49.5 ± 1.96 %.

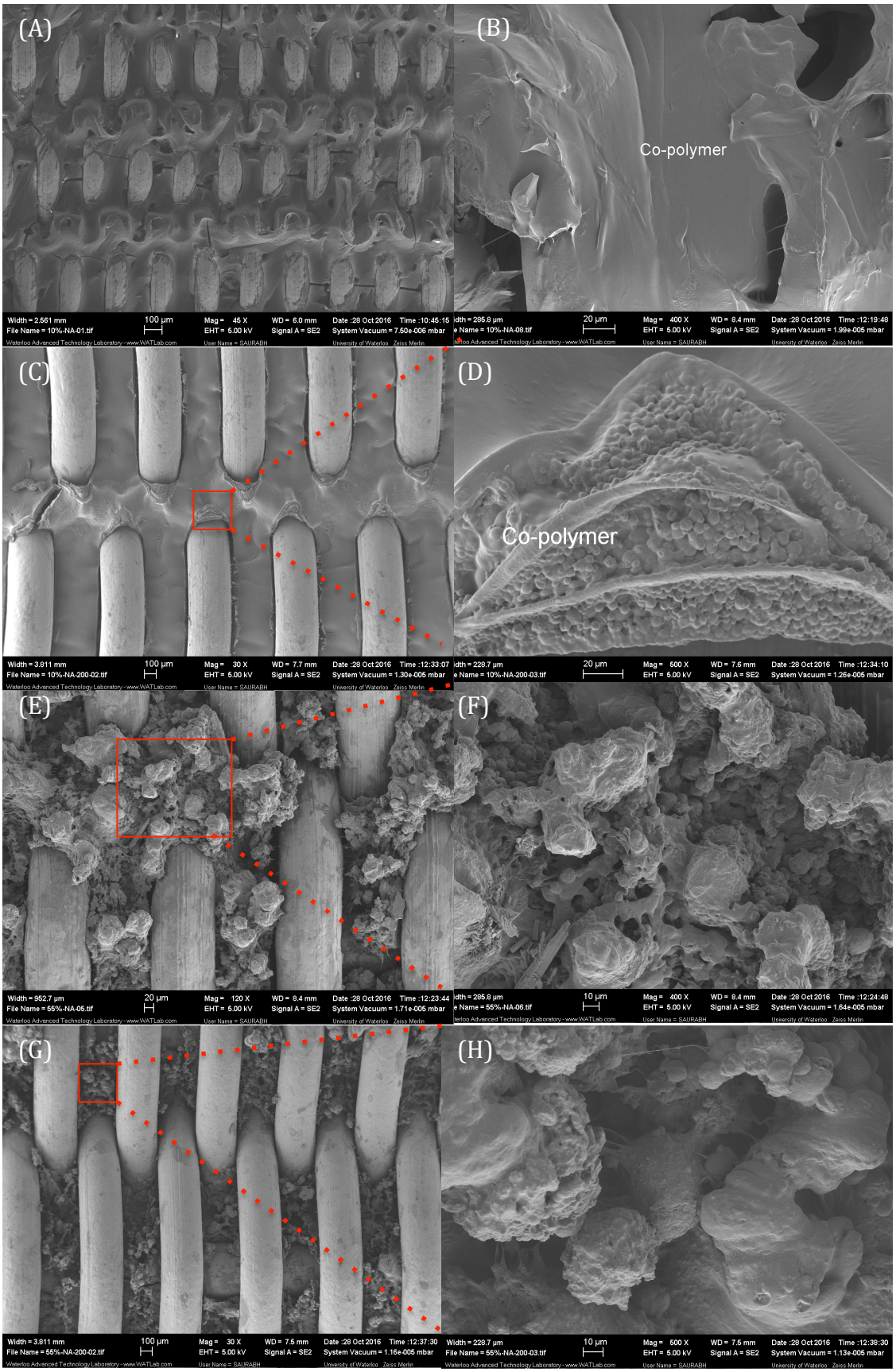
(A)
(B)
Co-polymer
(C)
(D)
Co-polymer
(E)
(F)
(G)
(H)

Figure 4.19 Morphological structure of and Na-AC/AM copolymers (10 and 55 Na-AC %) coating mesh prepared from a stainless steel mesh with a pore diameter of 55 and 200 μm. A and C) are large-area view of the copolymer coating mesh with 10 % Na-AC coated on 55 and 200 micron meshes, respectively; B and D) morphological overview structure and cross-sectional of 10 % Na-AC copolymer. E and G) large and view of the coating mesh with 55 % Na-AC copolymer on 55 and 200 micron meshes, respectively; F) and H) large and enlarge area of coating 55 % Na-AC copolymer with higher-magnification images of the copolymer, which indicates the higher swelling of copolymer.

4.6 Separation of Phenol using PAM Hydrogel-Coated Mesh

We tried to separate phenol from water (10/90 wt. %) by using PAM hydrogel coated mesh. The measurements were done for one time for different concentration of monomer on different mesh size (55,65,80 and 200 micron), as a trial but did not work. Spectrophotometry was used to measure the unknown phenol % in water after separation. The result was that some phenol passed through the mesh and the separation efficiency increased with increasing monomer concentration. However, the efficiency was low and considered to be not worth it. Therefore, we conclude that PAM hydrogel coated mesh cannot be used for separation of phenol from water. Since phenol is polar it passed through the mesh along with the water. Figure 4.22 illustrates the separation efficiency of 10 % phenol with max 60 % based on AM 60%, and it decreased with the thinner coated mesh.

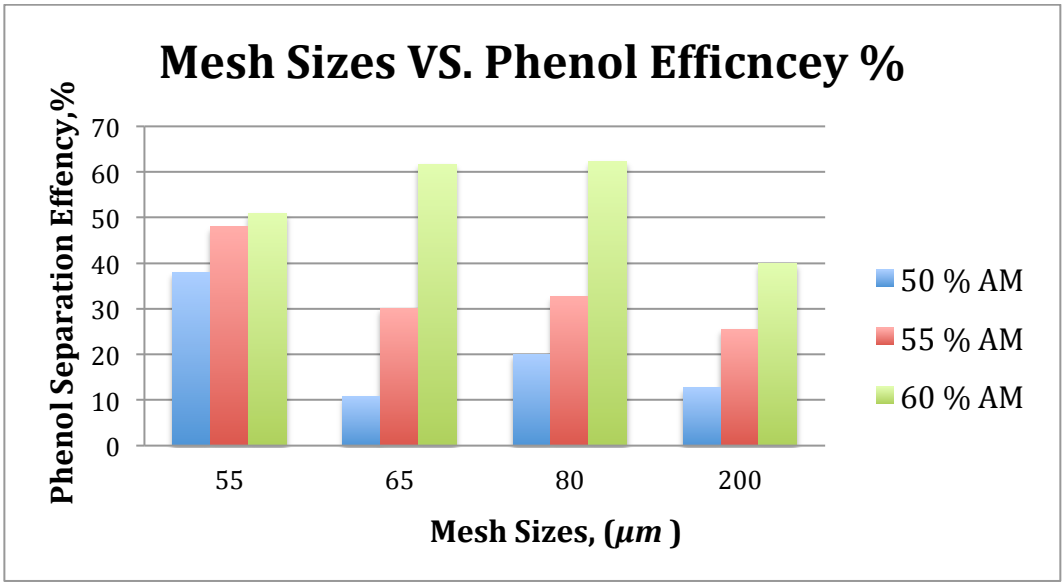

Figure 4.22. Separation efficiency of 10 % of phenol in water by PAM hydrogel coated meshes with three different AM content in PAM, which approved that PAM is not suitable to separate phenol from water.

Chapter 5: Conclusions and Recommendations

5.1 Conclusions

The results presented in this study demonstrate the effect of hydrogel-coated mesh on the separation of oil from water using a photon-initiated polymerization of the PAM polymer and Na-Ac/AM copolymer. On the basis of the results obtained throughout this work, the following conclusions can be stated:

(1) Water recovery ranged from 93 to 98 % for all mesh sizes and fluctuating based on the mesh sizes and monomer concentrations. The reasons for this high recovery being not 100 % are the higher possibility of water getting absorbed by the hydrogel, tightness of sealing, and adhesion force between water and glass tube.

(2) As the oil concentration in water increases, the separation efficiency decreases. This is equivalent to an increase in the pressure of oil, which allows passing of small amounts of oil through the pores. Therefore, Hydrogels work better with lower oil contents.

(3) The hydrogel coated mesh works by interacting differently with a species that is both hydrophobic and hydrophilic which was proved by measuring the contact angle of water in air which was less than 5° on the coated mesh. PAM polymer and Na-Ac/AM copolymer hydrogel coated meshes are super-hydrophilic in an air-solid-liquid three phases with both the contact angle of oil and water lower than 15 degree. Under-water, PAM hydrogel coated mesh become highly repulsive for oil, which was confirm from underwater OCAs of the four different size of meshes that are found to be greater than 90 degree, which indicate the hydrophobic properties of the coated mesh under water. This means that the oil cannot penetrate through the coated mesh while water is absorbed through the mesh.

(4) The difference in the water flow or separation time becomes smaller with increasing the mesh's pore size up to 80 micron, while separation time was higher for 200 micron mesh as more hydrogel was blocking the pores. In contrast, the separation time was faster with the copolymer due to the higher swelling capacity of the copolymer. Therefore, under-water oleo-phobic properties of the PAM coated mesh make it a promising technology for many applications, such as for wastewater treatment.

(5) HCP measurements proved that hydrogel gets thicker with increasing total monomer concentration. Hydrogel with low monomer content was thinner than with a higher monomer concentration, and the separation time is faster but separation efficiency is less than that of thicker hydrogel.

(6) Copolymer Na-Ac/AM with 55 % Na-Ac had the highest swelling capacity, and homo-polymer 50 % AM had the lowest swelling capacity.

(7) SEM images were used to prove the effected of the monomer concentration on the separation efficiency of the polymer and copolymer that affect also the swelling index.

5.2 Future Work and Recommendations

- In this work, only two levels of Na-AM feed composition were synthesized and tested. For more understanding of swelling mechanism, more experiments with different feed compositions should be investigated.
- For more applications in different industries, further experimentation with various oils and mesh sizes is recommended. Moreover, it is also recommended to try different applications such as separation of Sodium Chloride from water by using PAM, PAM plus CNT's and PAM-CNT's plus an additive such as Silicon

hydrogel-coated mesh to minimize the salt to get more separation efficiency.

- As stainless steel mesh was used for mechanical support, a biodegradable mesh made of coconut fibers or plain fibers can replace this. It would be biodegradable, environmentally friendly, lighter and cheaper than steel and at the same times ensures strength required for liquid/liquid separation applications.
- Since phenol is polar it passed through the mesh along with the water. As the phenol is polar it may react with the polymer, therefore it is recommended that adding additives like silicon to the polymer might prevent phenol from reacting with the polymer.

References:

1. Technology could solve longstanding problem of separating gas from water. Available at: http://phys.org/news/2016-03-technology-longstanding-problem-gas.html. (Accessed: 25th April 2016)
2. Pichtel, J. & Pichtel, J. Oil and Gas Production Wastewater: Soil Contamination and Pollution Prevention, Oil and Gas Production Wastewater: Soil Contamination and Pollution Prevention. *Appl. Environ. Soil Sci. Appl. Environ. Soil Sci.* **2016, 2016,** e2707989 (2016).
3. Ahmed, E. M. Hydrogel: Preparation, characterization, and applications: A review. *J. Adv. Res.* **6,** 105–121 (2015).
4. H. Gulrez, S. K., Al-Assaf, S. & O, G. in *Progress in Molecular and Environmental Bioengineering - From Analysis and Modeling to Technology Applications* (ed. Carpi, A.) (InTech, 2011).
5. Rosiak, J. M. & Yoshii, F. Hydrogels and their medical applications. *Nucl. Inst Methods Phys. Res. B* **151,** 56–64 (1999).
6. Schmedlen, R. H., Masters, K. S. & West, J. L. Photocrosslinkable polyvinyl alcohol hydrogels that can be modified with cell adhesion peptides for use in tissue engineering. *Biomaterials* **23,** 4325–4332 (2002).
7. Hoare, T. R. & Kohane, D. S. Hydrogels in drug delivery: Progress and challenges. *Polymer* **49,** 1993–2007 (2008).
8. Zhao, L. *Removal of Heavy Metals from Wastewater by Adsorption Using Chitosan Membranes*. (University of Waterloo, 2004).
9. Atta, A. M., Ismail, H. S. & Elsaaed, A. M. Application of anionic acrylamide-based hydrogels in the removal of heavy metals from waste water. *J. Appl. Polym. Sci.* **123,** 2500–2510 (2012).

10. Xue, Z. *et al.* A Novel Superhydrophilic and Underwater Superoleophobic Hydrogel-Coated Mesh for Oil/Water Separation. *Adv. Mater.* **23,** 4270–4273 (2011).

11. Fan, J.-B. *et al.* Directly Coating Hydrogel on Filter Paper for Effective Oil–Water Separation in Highly Acidic, Alkaline, and Salty Environment. *Adv. Funct. Mater.* **25,** 5368–5375 (2015).

12. Wen, Q., Di, J., Jiang, L., Yu, J. & Xu, R. Zeolite-coated mesh film for efficient oil–water separation. *Chem. Sci.* **4,** 591–595 (2013).

13. Bjorneberg, D. L. *Temperature, concentration, and pumping effects on PAM viscosity*. (1998).

14. Wever, D. A. Z., Picchioni, F. & Broekhuis, A. A. Polymers for enhanced oil recovery: A paradigm for structure–property relationship in aqueous solution. *Prog. Polym. Sci.* **36,** 1558–1628 (2011).

15. Rudin, A. *Elements of Polymer Science & Engineering: An Introductory Text and Reference for Engineers and Chemists*. (Academic Press, 1998).

16. Arthur, J. Daniel, Bruce G. Langhus, and Chirag Patel. 'Technical summary of oil & gas produced water treatment technologies.' All Consulting, LLC, Tulsa, OK (2005).

17. Zhang, F. *et al.* Nanowire-Haired Inorganic Membranes with Superhydrophilicity and Underwater Ultralow Adhesive Superoleophobicity for High-Efficiency Oil/Water Separation. *Adv. Mater.* **25,** 4192–4198 (2013).

18. Chiba, K. *et al.* Super water- and highly oil-repellent films made of fluorinated poly(alkylpyrroles). *Colloids Surf. Physicochem. Eng. Asp.* **354,** 234–239 (2010).

19. Yan, H., Kurogi, K. & Tsujii, K. High oil-repellent poly(alkylpyrrole) films coated with fluorinated alkylsilane by a facile way. *Colloids Surf. Physicochem. Eng. Asp.* **292,** 27–31 (2007).

20. Wang, H., Xue, Y. & Lin, T. One-step vapour-phase formation of patternable, electrically conductive, superamphiphobic coatings on fibrous materials. *Soft Matter* **7,** 8158–8161 (2011).

21. Jin, M. *et al.* Underwater Oil Capture by a Three-Dimensional Network Architectured Organosilane Surface. *Adv. Mater.* **23,** 2861–2864 (2011).

22. Jung, Y. C. & Bhushan, B. Wetting behavior of water and oil droplets in three-phase interfaces for hydrophobicity/philicity and oleophobicity/philicity. *Langmuir ACS J. Surf. Colloids* **25,** 14165–14173 (2009).

23. Xue, Z., Liu, M. & Jiang, L. Recent developments in polymeric superoleophobic surfaces. *J. Polym. Sci. Part B Polym. Phys.* **50,** 1209–1224 (2012).

24. Ding, C. *et al.* PANI nanowire film with underwater superoleophobicity and potential-modulated tunable adhesion for no loss oil droplet transport. *Soft Matter* **8,** 9064–9068 (2012).

25. Gao, X. *et al.* Dual-Scaled Porous Nitrocellulose Membranes with Underwater Superoleophobicity for Highly Efficient Oil/Water Separation. *Adv. Mater.* **26,** 1771–1775 (2014).

26. Tian, D. *et al.* Photo-induced water–oil separation based on switchable superhydrophobicity–superhydrophilicity and underwater superoleophobicity of the aligned ZnO nanorod array-coated mesh films. *J. Mater. Chem.* **22,** 19652–19657 (2012).

27. Zhang, M., Zhang, T. & Cui, T. Wettability conversion from superoleophobic to superhydrophilic on titania/single-walled carbon nanotube composite coatings. *Langmuir ACS J. Surf. Colloids* **27,** 9295–9301 (2011).

28. Chhatre, S. S. *et al.* Scale Dependence of Omniphobic Mesh Surfaces. *Langmuir* **26,** 4027–4035 (2010).

29. Yang, J., Zhang, Z., Men, X., Xu, X. & Zhu, X. A simple approach to fabricate superoleophobic coatings. *New J. Chem.* **35,** 576–580 (2011).

30. Huang, J., Huang, Y., He, C. & Gao, Y. Synthesis and characterization of photoresponsive POSS-based polymers and their switchable water and oil wettability on cotton fabric. *RSC Adv.* **5,** 100339–100346 (2015).

31. Feng, L. *et al.* A Super-Hydrophobic and Super-Oleophilic Coating Mesh Film for the Separation of Oil and Water. *Angew. Chem.* **116,** 2046–2048 (2004).

32. Mohana Raju, K. & Padmanabha Raju, M. Synthesis of novel superabsorbing copolymers for agricultural and horticultural applications. *Polym. Int.* **50,** 946–951 (2001).

33. ZHOU, M., LI Qian & Jiping, X. STUDY ON ACRYLAMIDE-SODIUM ACRYLATE COPOLYMER GELS. *Chin. J. Polym. Sci. CJPS* **8,** (1990).

34. Karadağ, E. & Saraydin, D. Swelling of Superabsorbent Acrylamide/Sodium Acrylate Hydrogels Prepared Using Multifunctional Crosslinkers. *Turk. J. Chem.* **26,** 863–876 (2002).

35. Lee, W.-F. & Yuan, W.-Y. Thermoreversible hydrogels X: Synthesis and swelling behavior of the (N-isopropylacrylamide-co-sodium 2-acrylamido-2-methylpropyl sulfonate) copolymeric hydrogels. *J. Appl. Polym. Sci.* **77,** 1760–1768 (2000).

36. Kalaleh, H.-A., Tally, M. & Atassi, Y. Preparation of poly(sodium acrylate-co-acrylamide) superabsorbent copolymer via alkaline hydrolysis of acrylamide using microwave irradiation. *ArXiv150203639 Cond-Mat* (2015).

37. Shukla, N. B. & Madras, G. Photo, thermal, and ultrasonic degradation of EGDMA-crosslinked poly(acrylic acid-co-sodium acrylate-co-acrylamide) superabsorbents. *J. Appl. Polym. Sci.* **125,** 630–639 (2012).

38. Roger, P., Gérard, S., Burckbuchler, V., Renaudie, L. & Judeinstein, P. Effect of the incorporation of a low amount of carbohydrate-containing monomer on the swelling properties of polyacrylamide hydrogels. *Polymer* **48,** 7539–7545 (2007).

39. El-Hag Ali, A., Shawky, H. A., Abd El Rehim, H. A. & Hegazy, E. A. Synthesis and characterization of PVP/AAc copolymer hydrogel and its applications in the removal of heavy metals from aqueous solution. *Eur. Polym. J.* **39,** 2337–2344 (2003).

40. Krušić, M. K., Milosavljević, N., Debeljković, A., Üzüm, Ö. B. & Karadağ, E. Removal of Pb2+ Ions from Water by Poly(Acrylamide-co-Sodium Methacrylate) Hydrogels. *Water. Air. Soil Pollut.* **223,** 4355–4368 (2012).

41. Cinnirella, S., Hedgecock, I. M. & Sprovieri, F. Heavy metals in the environment: sources, interactions and human health. *Environ. Sci. Pollut. Res.* **21,** 3997–3998 (2014).

42. Kim, S.-J. *et al.* Removal of heavy metal-cyanide complexes by ion exchange. *Korean J. Chem. Eng.* **19,** 1078–1084

43. Balasim A.AbiD, M. M. B. & Najah M. Al-ShuwaikI. Removal of Heavy Metals Using Chemicals Precipitation. *Eng Tch J.* **29,** (2010).

44. Magalhães, A. S. G. *et al.* Application of ftir in the determination of acrylate content in poly(sodium acrylate-co-acrylamide) superabsorbent hydrogels. *Quím. Nova* **35,** 1464–1467 (2012).

45. Candau, F., Zekhnini, Z. & Durand, J. in *New Trends in Colloid Science* (ed. Hoffmann, H.) 33–36 (Steinkopff, 1987).

46. Armenta, S., Moros, J., Garrigues, S. & de la Guardia Cirugeda, M. in *Olives and Olive Oil in Health and Disease Prevention* (ed. Watson, R. R.) 533–544 (Academic Press, 2010).

47. Yang, M. in *Produced Water* (eds. Lee, K. & Neff, J.) 57–88 (Springer New York, 2011).

48. Rainwater, F. H. & Thatcher, L. L. *Methods for Collection and Analysis of Water Samples*. (U.S. Government Printing Office, 1960).

49. Gomez, N. A., Abonia, R., Cadavid, H. & Vargas, I. H. Chemical and spectroscopic characterization of a vegetable oil used as dielectric coolant in distribution transformers. *J. Braz. Chem. Soc.* **22,** 2292–2303 (2011).

50. *Wilcox, J. R.; Cavins, J. F.; Nielsen, N. C.; J. Am. Oil Chem. Soc. 1984, 61, 97.*

51. Encinas, M. V.; Lissi, E. A.; Rufs, A. M.; Altamirano, M.; Cosa, J. J.; Photochem. Photobiol. 1998, 68, 447; Smirnoff, N.; New Phytol. 1993, 125, 27.

52. Fisher, L. R., Mitchell, E. E. & Parker, N. S. Interfacial Tensions of Commercial Vegetable Oils with Water. *J. Food Sci.* **50,** 1201–1202 (1985).

53. Zhang, L., Zhang, Z. & Wang, P. Smart surfaces with switchable superoleophilicity and superoleophobicity in aqueous media: toward controllable oil/water separation. *NPG Asia Mater.* **4,** e8 (2012).

54. Yao, K.-J. & Zhou, W.-J. Synthesis and water absorbency of the copolymer of acrylamide with anionic monomers. *J. Appl. Polym. Sci.* **53,** 1533–1538 (1994).

55. Kang, W. *et al.* Solution behavior of two novel anionic polyacrylamide copolymers hydrophobically modified with *n* -benzyl- *n* -octylacrylamide. *Polym. Eng. Sci.* **52,** 2688–2694 (2012).

56. Bin, Z., Hu, H., Chen, M. & Liu, W. Synthesis of associating poly(acrylic acid) in supercritical carbon dioxide and its solution properties. *Colloid Polym. Sci.* **282,** 1228–1235 (2004).